UNCLASSIFIED

AD NUMBER

AD860696

NEW LIMITATION CHANGE

TO

Approved for public release, distribution unlimited

FROM

Distribution authorized to U.S. Gov't. agencies and their contractors; Critical Technology; 23 JUN 1969. Other requests shall be referred to Naval Avionics Facility, Indianapolis, IN 46218.

AUTHORITY

usnafi ltr, 10 may 1972

THIS PAGE IS UNCLASSIFIED

AD 860696

TR 1331
23 JUNE 1969

NAFI publication

APPLIED RESEARCH DEPARTMENT

SERVO AMPLIFIER /SERVOMOTOR COMPATIBILITY STUDY

THIS DOCUMENT IS SUBJECT TO SPECIAL EXPORT CONTROLS AND EACH TRANSMITTAL TO FOREIGN GOVERNMENTS OR FOREIGN NATIONALS MAY BE MADE ONLY WITH PRIOR APPROVAL OF NAVAL AVIONICS FACILITY, INDIANAPOLIS, INDIANA

DDC
RELEASED
OCT 30 1969

NAVAL AVIONICS FACILITY
INDIANAPOLIS, INDIANA 46218

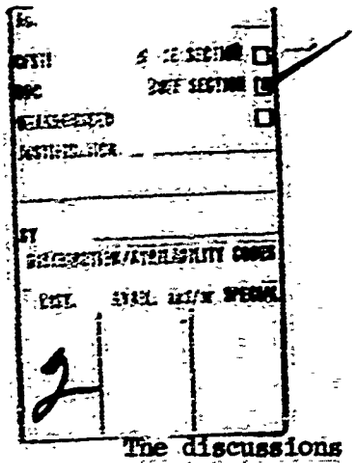

NOTICES

The discussions or opinions concerning commercial products herein do not constitute an endorsement or condemnation by the government, nor do they convey or imply the right to a license for use of such products.

PREFACE

The purpose of this study was to establish a criterion which could be used to predict the stability performance of servo amplifier/servomotor combinations. A particular amplifier/motor combination is defined as unstable when there are oscillations in the amplifier output voltage due to the effect of the servomotor impedance on the amplifier internal feedback loop. These oscillations are not to be confused with those of a servo system.

This study develops a technique to obtain the open-loop gain characteristics of servo amplifiers by means of external measurements with no access to the feedback loop and no knowledge of the exact amplifier circuit configuration. With this technique and proper specifications on the servomotor, a worst-case stability dummy load can be specified for testing the stability characteristics of incoming production servo amplifiers. The theory, procedures, and test techniques necessary to obtain the worst-case loads are presented. Amplifier loop gain and load impedance frequency characteristics are examined to determine the frequency range where instability may occur. Specialized computer programs written to aid in the stability determinations are included for future reference. A limited number of servo amplifiers were evaluated, and the results are summarized. Recommendations are made to modify present specifications to include parameters which will insure the stable operation of amplifier/motor combinations.

This work was performed under AIRTASKS A34520/2311/69F17532402 and A34522006/2311/F008-01-15 for Naval Air Systems Command (AIR-52022).

ABSTRACT

This report presents a study of the stability problem (tendency for unwanted oscillation) of a servo amplifier driving a servomotor. Servo amplifier stability is affected by the servomotor impedance being reflected back into the amplifier internal feedback loop.

The servo amplifier/servomotor modeling techniques used for stability evaluation are considered. The study develops techniques for evaluating, testing, and specifying servo amplifier/servomotor combinations with respect to stability. Recommendations are made to modify present specifications to include parameters which will insure stable operation of amplifier/motor combinations. A limited number of commercially available servo amplifiers with standard servomotors are evaluated and results are summarized.

Prepared By: Clifford E. Hogue
CLIFFORD E. HOGUE

Leonard S. Skwiera
LEONARD S. SKWIERA

Jack W. Templeton
JACK W. TEMPLETON

Approved By: Ronald R. Jennings
RONALD R. JENNINGS, Chief
Controls Systems Branch

F. J. Jewell for
FRANCIS A. MARASCO, Manager of
Experimental Research Division

TABLE OF CONTENTS

		Page
	PREFACE	ii
	ABSTRACT	iii
	LIST OF FIGURES	vi
	LIST OF TABLES	vii
	GLOSSARY OF MOTOR MODEL TERMS	viii
I.	CONCLUSIONS	1
II.	RECOMMENDATIONS	3
	A. DUMMY LOAD USAGE	3
	B. SERVOMOTOR SPECIFICATION CHANGES	4
III.	INTRODUCTION	7
	A. STATEMENT OF PROBLEM	7
	B. GENERAL DESCRIPTION OF SERVO AMPLIFIER/SERVOMOTOR OPERATION	8
IV.	SERVO AMPLIFIER/SERVOMOTOR COMPATIBILITY WITH RESPECT TO SPECIFICATIONS AND PRODUCTION TESTING	11
V.	SERVOMOTOR DISCUSSION	15
	A. SERVOMOTOR DESCRIPTION	15
	B. EQUIVALENT SERIES CIRCUIT PARAMETER CORRELATION	18
	C. COMPLEX EQUIVALENT CIRCUIT PARAMETER DETERMINATION	26
VI.	SERVO AMPLIFIER DISCUSSION	36
	A. GENERAL DESCRIPTION	36
	B. GH OBTAINED BY EXTERNAL MEASUREMENT	37
	C. HOW TO OBTAIN Z_{11} and Z_{12} (unstable) CURVES FROM GH CURVES	38
	D. CURVE COMPARISON	46
VII.	STABILITY DETERMINATION TECHNIQUES	48
	A. DUMMY LOAD DETERMINATION	48
	B. TESTING PROCEDURE (AMPLIFIER WITH WORST-CASE DUMMY LOAD)	66
	C. COMPARISON OF PLOTS Z (unstable) AND Z_{12} FOR WORST-CASE STABILITY DUMMY LOAD	66
	D. COMPARISON OF THE RESULTS OF THE TWO STABILITY DETERMINATION TECHNIQUES	68

TABLE OF CONTENTS (Continued)

		Page
VIII.	EVALUATION OF SERVO AMPLIFIER PERFORMANCE	75
	A. CRITERIA FOR EVALUATION OF SERVO AMPLIFIER/SERVOMOTOR COMBINATIONS	75
	B. SUMMARY OF TEST RESULTS	79
	C. SUMMARY OF SERVO AMPLIFIER PERFORMANCE	79
	DISTRIBUTION LIST	81

LIST OF FIGURES

Figure		Page
1a.	Servo Amplifier Flow Graph	9
1b.	Servo Amplifier Simplified Schematic	10
2.	Servo Amplifier Equivalent Circuit	13
3.	Equivalent Series Motor Model	15
4.	Complex Equivalent Circuit of the Servomotor	16
5.	Ideal Dummy Load for the Complex Motor Model	17
6.	Plot of R_S Versus X_{LS} for Several Motor Samples	19
7.	Plot of R_{DC} Versus X_{LS} for Several Motor Samples	27
8.	Matrix of Possible Combinations of Extreme Motor Parameters	28
9.	Servomotor Impedance Determination	29
10.	Time-Sharing Computer Program for Calculation of Motor Impedances Z_1 and Z_3	30
11.	Calculated Values of Motor Impedances Z_1 and Z_3	31
12.	Bode Plots of Z_1 and Z_3	33
13.	Equivalent Servomotor Circuits	34
14.	Flow Diagrams of a Single Loop Amplifier	38
15.	Flow Diagrams of a Multiloop Amplifier	39
16.	Flow Diagrams of an Amplifier with Internal Loop	40
17.	Output Impedance Measurement Circuit	41
18.	Flow Chart for Computation of GH and $Z_{unstable}$	42
19.	Card FORTRAN Computer Program for Computation of GH and $Z_{unstable}$	43
20.	Time-Sharing BASIC Computer Program for Computation of GH and $Z_{unstable}$	44
21.	Comparison of Z_{1a} and $Z_{unstable}$ Curves to Determine Stability	47
22.	Printout of Program to Calculate Load Impedances Z_{11} and Z_{12} (Card FORTRAN Version)	51
23.	Printout of Program to Calculate Load Impedances Z_{11} and Z_{12} (Time-Sharing BASIC Version)	52
24.	Computer Printout of Performance and Construction Data for the Transformer Design	56

LIST OF FIGURES (Continued)

Figure		Page
25a, b.	Comparison of Z_{12} Responses	60, 61
26.	Practical Dummy Load for the Complex Equivalent Circuit Motor Model	62
27.	Experimental Dummy Load for the Equivalent Circuit Motor Model	63
28a.	Practical Equivalent Series Dummy Load	64
28b.	Ideal Equivalent Series Dummy Load	65
29.	Nyquist Plots	68
30.	Stable X-Y Plot	76
31.	Low Level Oscillating X-Y Plot	77
32.	High Level Oscillating X-Y Plot	78

LIST OF TABLES

I.	Coordinates of the Corners of the Parallelograms Defining Regions of Acceptable Motor Parameter Combinations	6
II.	Least Squares Best Linear Fit Equations	6
III.	Servomotors	21
IV.	Servomotor Equivalent Series Circuit Parameters Obtained from Kearfott and NAD, Crane, Indiana	23
V.	Servomotor Equivalent Circuit Parameters for Motors Tested at NAFI	25
VI.	Definition of Variables Used in Computation of GH and ZL (unstable)	45
VII.	Worst-Case Dummy Loads	50
VIII.	Definition of Variables Used in the Computation of Z_{11} and Z_{12}	53
IX.	Parameter Limits for Worst-Case Power Dummy Loads	55
X.	Servo Amplifiers Tested	69
XI.	Transfer Function Plot Characteristics	71
XII.	Correlation of Stability Tests	73
XIII.	Summary of Amplifier Stability	80

GLOSSARY OF MOTOR MODEL TERMS

$R_S = R_{AC} + R_{DC}$ -- Series Resistive component of the complex impedance

R_{AC} ---------- Serie. AC resistance

R_{DC} ---------- DC resistance of the stator or stator copper loss

L_S ---------- Series Inductive component of the complex impedance

X_{LS} ---------- Series Reactive component of the complex impedance

L_{LS} ---------- Stator leakage inductance

L_{LR} ---------- Rotor leakage inductance

$L = L_M$ --------- Magnetizing inductance

R_M ---------- Core loss

R_R ---------- Rotor Resistance

S ---------- Slip

R_R/S ---------- Effective rotor resistance

$\frac{L_{LP}}{2}$ ---------- Leakage inductance in half the primary (stator) which is not magnetically coupled to the other half of the primary winding.

Series Motor Model - A simple model of the servomotor in which the impedance of the control winding is lumped into three series components: R_{DC}, R_{AC}, and L_S.

Complex Motor Model - A more realistic model of the servomotor in which the inductive coupling between the stator and the rotor of the motor is represented by a symmetric transformer equivalent.

Ideal Equivalent Circuit - An equivalent circuit of the servomotor which was developed theoretically and does not take into consideration parasitics associated with the actual components which will be used to implement the circuit for laboratory testing.

Practical Equivalent Circuits - An extension of the Ideal Equivalent Circuit which includes models for the physical components (and their associated parasitics) used in the experimental dummy loads. These equivalent circuits were established and analyzed using the NAFI CODED circuit analysis program to verify the experimental data measured in the laboratory.

Experimental Equivalent Circuit - An equivalent circuit which schematically represents the configuration of the actual physical components

utilized in the dummy load for laboratory tests.

EQUIVALENT CIRCUIT	SERIES MODEL	COMPLEX MODEL
Ideal	Fig. 28b Page 65	Fig. 5 Page 17
Practical	Fig. 28a Page 64	Fig. 26 Page 62
Experimental	Fig. 28b Page 65	Fig. 27 Page 63
	Similar to Ideal Circuit	

I. CONCLUSIONS

A. Present servo amplifier and servomotor specifications are not sufficient to insure the stable operation of the combination. Many amplifier specifications do not present the range of loads which will result in stable amplifier operation. The effects of the frequency characteristics of the load on the amplifier loop gain are not considered. The servomotor specifications do not usually mention parameters which are important for stability considerations, such as the control winding DC resistance, and the leakage reactance between the halves of the control winding.

B. The standard series equivalent circuit motor model (Fig. 3, page 15) is not sufficient to determine the stability characteristics of a servomotor/servo amplifier combination. This motor model does not simulate the frequency characteristics of the motor except at the operating frequency (400 Hz).

C. The standard series equivalent circuit motor model including the control winding DC resistance (R_{DC}), the leakage reactance (X_{LLP}) and the equivalent transformer between the halves of the control winding (Fig. 28b, page 65) is sufficient to simulate the motor characteristics and to determine the stability performance of the amplifier/motor combinations at frequencies above the operating frequency (400 Hz). For the limited number of amplifiers tested, it was observed that all instabilities occured at frequencies above 400 Hertz. In general, however, the equivalent series motor model would not be sufficient to test for amplifier/motor combination instabilities because oscillations could occur at frequencies below 400 Hertz.

D. The complex equivalent circuit motor model (Fig. 5 page 17) is sufficient to simulate the frequency characteristics of the servomotors both above and below the operating frequency.

E. Given no external access to servo amplifier feedback loops and no knowledge of the circuit configuration, it is possible by an external measurement technique to obtain the loop gain characteristics of an amplifier. The only requirement necessary for this technique to be valid is that there be feedback connected to one of the output terminals. This is typical, since low output impedance and gain stability are desired and achieved by this feedback connection.

F. The stability performance of a servo amplifier/servomotor combination can be established by a worst-case stability dummy load test.

G. The power output capability of a servo amplifier can be established by a worst-case power dummy load test.

H. A nominal worst-case dummy load can be established for evaluating servo amplifier phase shift, gain magnitude, gain linearity, and saturated output voltage by means of transfer function plots.

I. A technique is necessary to establish the correlation between the values of R_{DC} and L_S and between the values of R_S and L_S in order to determine realistic limits for a worst-case dummy load. (See Fig. 3, page 15, for definitions.)

J. A measurement technique was necessary to obtain R_{DC} and L_L, since these parameters were not specified.

K. The stability of servo amplifiers is very sensitive to proper signal and power ground connections. The large power ground currents must not flow through the input signal ground lead.

L. Proper heat-sinking of a servo amplifier is very important since the amplifier tends toward instability with increasing temperature.

M. The choice of a dummy load for an amplifier depends on the internal circuit configuration and open loop gain characteristics of the amplifier.

II. RECOMMENDATIONS

A. DUMMY LOAD USAGE

Servo amplifier procurement should incorporate testing with worst-case dummy loads to establish more accurate and complete amplifier performance data. It is recommended that three separate dummy loads be utilized. A nominal dummy load should be utilized to obtain amplifier room temperature performance data such as gain magnitude, gain linearity, phase shift, and saturated output voltage level.

The second load is the worst-case stability dummy load. This load should represent the worst set of amplifier load parameters which would tend to cause oscillations in the amplifier output voltage. The amplifier should be at high temperature when tested with this load to establish a worst-case stability condition. The dummy load may be designed for use at room temperature by having all its temperature-dependent parameters altered to simulate a motor at the worst-case high temperature.

The third load that should be used is the worst-case power dummy load. All of the temperature conditions and load parameter values should be chosen to provide a load which will produce minimum in-phase power delivered to the load.

It is suggested that the complex motor model (Fig. 5, page 17) be used for the worst-case stability dummy load. The parameters which must have their ranges specified to determine the simpler equivalent series motor model (Fig. 28b, page 65) are R_s, L_s, R_{DC}, L_{LP}. The coupling coefficient, K, between the stator and rotor of the servomotor is the only additional parameter needed to obtain the complex model parameters from the equivalent series model data. Preliminary calculations from the limited amount of testing performed indicate that only the value of K has a secondary effect on the motor impedance (Z_{12}) and, consequently, on the stability in the frequency regions where instability is likely to occur. Therefore, it is recommended that only the parameters for the equivalent series motor model (R_s, L_s, R_{DC}, and L_{LP}) be required on the motor specification. The value of K should then be determined by the method presented in the report when worst-case dummy loads are being developed.

B. SERVOMOTOR SPECIFICATION CHANGES

Servomotor specifications should include the maximum value of the leakage inductance between the halves of the control winding (L_{LP}) and the range of values of the control winding DC resistance (R_{DC}) as defined in Figure 28b, page 65. The technique presented in this report to measure these recommended motor parameters should be utilized.

In order to develop a worst-case dummy load from a motor specification, bounds must be placed on motor parameter values. Using the data available (about 30 samples for each size motor), bounds were placed on the motor parameters. It was observed that realistic bounds could only be established when correlation between certain motor parameters are taken into account. The value of the control winding series reactance (X_{LS}) is correlated with the control winding total series resistance (R_S) and DC resistance (R_{DC}). Since X_{LS} is the motor parameter which had the minimum value distribution spread about the sample average, it was chosen as the independent variable for the correlation. Thus, for every value of X_{LS}, there exist ranges of the values of R_S or R_{DC}. The region of acceptable motor parameter combinations on a plot of X_{LS} versus either R_S or R_{DC} would be a parallelogram rather than the square region obtained when all parameters are considered to be independent of each other.

It is recommended that similar testing on larger sample sizes be performed to establish more accurate correlation and data spread information for the motors. However, using the limited sample sizes available for this study, specifications for all the motor parameters were determined. The values of X_{LS} all fell within a range of ± 15% around the sample average. The least squares best linear fit curve was drawn on the plots of X_{LS} versus R_S and R_{DC}. The allowable spread of R_S and R_{DC} values for any particular value of X_{LS} was assumed to be ± 15% (of R_S and R_{DC} sample averages) around the best linear fit curves. Table I provides the coordinates of the corners of the parallelograms defining regions of acceptable motor parameters on the X_{LS} versus R_S or R_{DC} plots. The equations for the least squares best linear fit correlation relationships

between parameter data sets are given in Table II. Out of the total of 80 motor data sets available, only the data for two motors did not fall within the parallelograms.

In addition to specifying X_{LS}, R_S, and R_{DC} using correlation techniques, the maximum value of the leakage inductance between the halves of the control winding (L_{LP}) should be specified. The largest value of L_{LP} is the worst-case as far as stability is concerned, and L_{LP} does not significantly affect the nominal or worst-case power dummy loads at 400 Hertz. A worst-case value of 2.6 mh was used to determine the dummy loads for the set of motors investigated. This value was slightly higher than the highest experimental value which was 1.8 mh.

TABLE I Coordinates of the Corners of the Parallelograms Defining Regions of Acceptable Motor Parameter Combinations

Motor Size	X_{LS} (Ohms)	R_{DC} Range* (Ohms)	R_S Range (Ohms)
8	160.6	64.3 - 91.1	96.9 - 141.7
	217.3	87.3 - 114.1	157.7 - 202.5
11	151.5	17.4 - 27.2	49.7 - 85.7
	205.0	37.9 - 47.7	157.6 - 194.2
15	81.7	6.8 - 10.6	33.5 - 51.3
	110.5	14.9 - 18.7	67.6 - 85.4

*R_{DC} measured at room temperature

TABLE II Least Squares Best Linear Fit Equations

Motor Size	Equations for Least Squares Best Linear Fit
8	$R_{DC} = 0.4057(X_{LS}) + 12.536$
8	$R_S = 1.0732(X_{LS}) - 53.083$
11	$R_{DC} = 0.3824(X_{LS}) - 35.625$
11	$R_S = 2.0296(X_{LS}) - 240.136$
15	$R_{DC} = 0.2790(X_{LS}) - 14.074$
15	$R_S = 1.1861(X_{LS}) - 54.529$

III. INTRODUCTION

A. STATEMENT OF PROBLEM

The basic problem and purpose of this report is best demonstrated by the following real life example. A servomechanism is designed and tested with a certain servo amplifier/servomotor combination in the control loop. The servo operates satisfactorily and meets all of the design specifications. Specifications are then drafted for the amplifier and motor and sent to manufacturers for bid. The contracts for the servo amplifiers and servomotors are awarded respectively to Company A and Company B. The system operates satisfactorily with this particular amplifier/motor combination. Upon completion of the original contract, the servo components are resubmitted for bid. Company C is awarded the contract for the servo amplifiers and Company B retains the contract for the servomotors. When this motor is connected to the amplifier, oscillation occurs. The oscillation normally occurs at some frequency above the specified operating frequency. This, of course, causes extremely expensive production delays and crash analysis studies to determine the cause of the problem.

This example problem points out the fact that present servomotor/servo amplifier specifications are not sufficient to insure the stable operation of amplifier/motor combinations. A sufficient set of specifications were established for the determination of amplifier/motor compatibility. In determining these specifications, the economics of increasing the price of the components due to additional specifications was kept in mind. Therefore, it was of prime consideration to keep the number of additional specifications to a minimum and to establish a testing technique which would not be costly in an inspection and production environment. The following ideas, reasonings, and solutions were used to develop a criterion which would insure the stable operation of servo amplifier/servomotor combinations. It is intended that the information contained in this report will be useful to both manufacturers and users of servo amplifiers and servomotors.

B. GENERAL DESCRIPTION OF SERVO AMPLIFIER/SERVOMOTOR OPERATION

Figures 1a and 1b illustrate typical servo amplifier/servomotor diagrams for an amplifier with a built-in 90° phase shift. A push-pull, usually Class B, output stage is employed. This type amplifier acts like two separate amplifiers operating on alternate half cycles of the carrier signal, with loop gains that are relatively independent of one another. The stability problem is due to the feedback required to obtain the desired amplifier characteristics of low output impedance and calibrated gain. The feedback loop is normally connected to one side of the output stage, and therefore, has different paths during different half-cycles of the carrier signal. It should be noted that the tuned motor load and the tuned interstage transformer are usually in the feedback loop.

Optimum performance and power transfer to the motor are attained by tuning the motor impedance for unity power factor at the carrier frequency. This is usually accomplished by a parallel tuning capacitor on the control winding. Although some stability advantage can be achieved with a parallel tuning capacitor on each half of the control winding (reference NAFI TR-1053), the continuing efforts toward small size and weight in military electronics favors the single capacitor tuning method. All motor tuning referenced in this report will mean single capacitor tuning unless otherwise specified.

The major consideration in this study is the determination of amplifier/motor compatibility with respect to stability. The advantages and disadvantages of the test methods are reviewed with respect to feasibility for use in a production environment.

A number of amplifiers and motors were tested to verify the theory presented. The results are given in Chapter VIII.

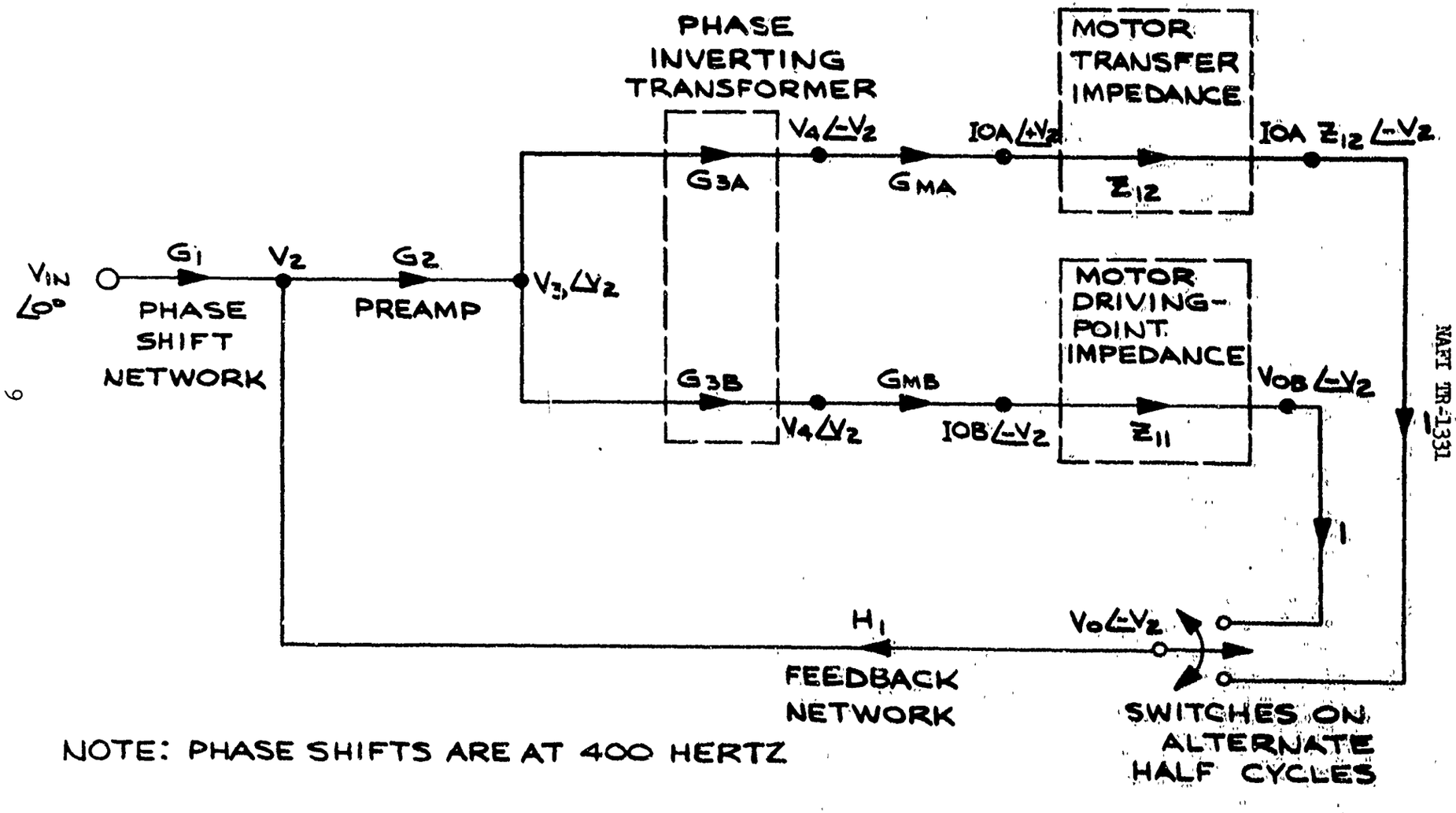

NOTE: PHASE SHIFTS ARE AT 400 HERTZ

FIG. 1a- SERVO AMPLIFIER FLOW GRAPH

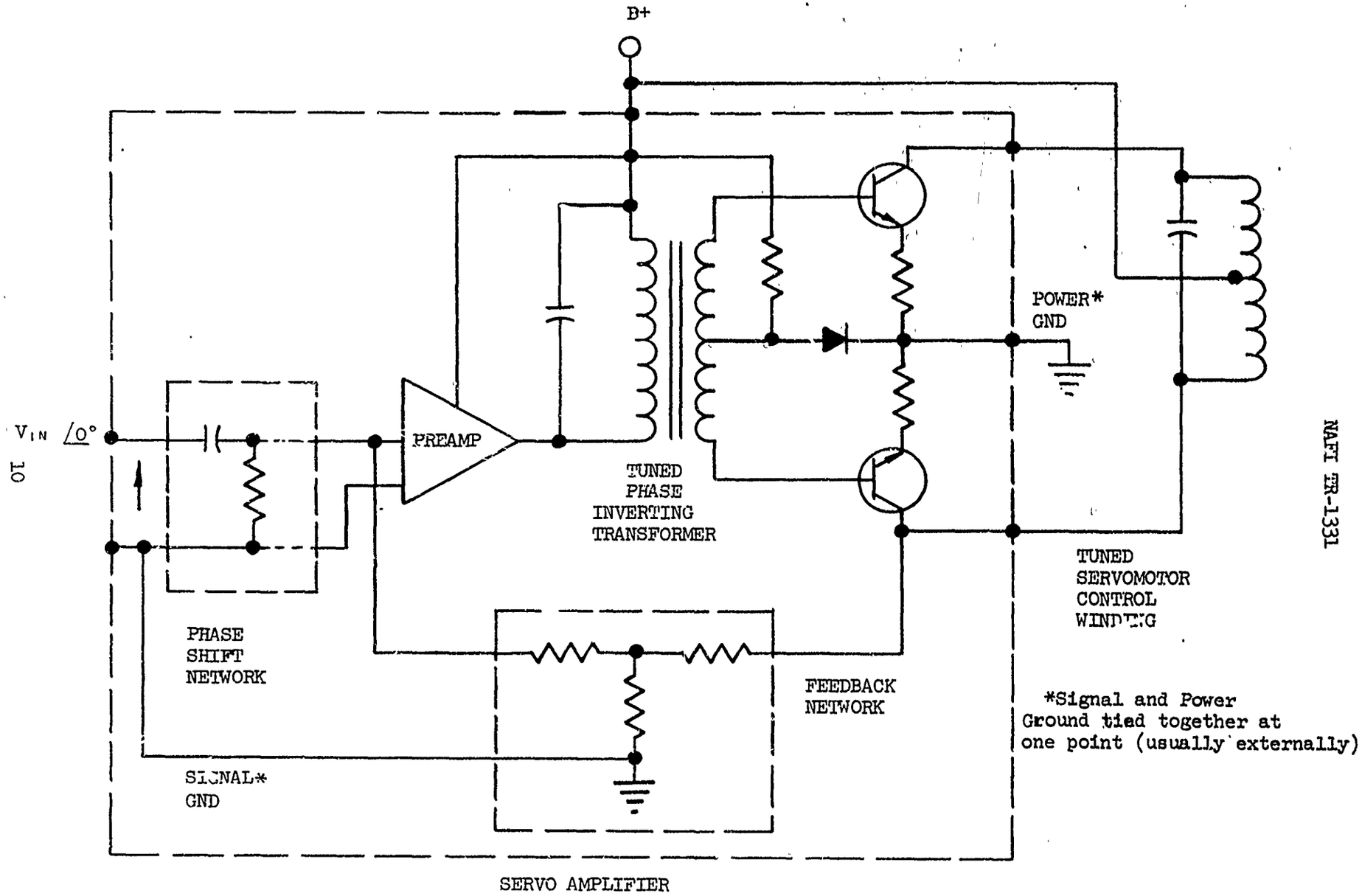

Figure 1b Servo Amplifier Simplified Schematic

NAFI TR-1331

IV. SERVO AMPLIFIER/SERVOMOTOR COMPATIBILITY WITH RESPECT TO SPECIFICATIONS AND PRODUCTION TESTING

As pointed out in the introduction, present servo amplifier/servomotor specifications are not sufficient to predict the stability performance of the combination. Present servo amplifier specifications state that the amplifiers are designed to operate into an effective impedance of XXX (ohms). This specification assumes that the load is basically inductive and tuned at the operating frequency by means of a parallel tuning capacitor. The specification in no way takes into account the stability characteristics of the amplifier over the entire frequency range of interest.

Present servomotor specifications call out nominal values of the series resistive component of the complex impedance (R_s) and the series reactive component of the complex impedance (X_{Ls}). These specifications are sufficient to specify a motor model that adequately simulates the characteristics of a servomotor at the operating frequency. It shall be demonstrated that a stability problem does not exist at the operating frequency, but at some value above the operating frequency. Because of this fact, the present servomotor specifications and models are not adequate to properly simulate the characteristics over the entire frequency range of interest.

The first consideration in determining stable operation of the amplifier/motor combination is to establish a method to predict the stability characteristics of the servo amplifier. In order to predict the stability performance, it is necessary to obtain the open-loop gain characteristics of the amplifier. The first method utilized consisted of performing a circuit analysis using the NAFI CODED (Computer Oriented Design of Electronic Devices) circuit analysis program on the amplifier/motor combination. This technique is not feasible in a production environment because the amplifier manufacturers are hesitant to release the actual circuit schematics which are of a proprietary nature. Even if the schematics were available, there is no guarantee that the manufacturer

will not change the circuit configuration in the middle of the contract so as to improve the circuit design and performance. For these reasons, this method of obtaining open-loop gain characteristics is not satisfactory in a production environment.

The second method of obtaining the open-loop gain characteristics of the amplifiers consists of obtaining a frequency response of the amplifier with the feedback loop opened. This method is also not feasible in a production environment since the amplifiers are totally encased and usually have no access to the feedback loop.

Since the amplifier internal circuitry cannot be determined nor usually specified, and since there is no access to the feedback loop, it is necessary to look at the characteristics of the amplifier from terminal (external) measurements. In general, any circuit with one or more feedback loops can be represented by an equivalent circuit with only one feedback loop. The equivalent circuit utilized in this study is illustrated in Figure 2. The parameters G, H, and open-loop output impedance ($Z_o(OL)$) are frequency dependent variables. Usually $Z_o(OL)$ is high compared to the load impedance and is neglected.

A method was devised to measure the GH product as a function of frequency and is presented in Chapter VI. From the values of the GH magnitude and angle at each frequency, a load could be calculated that would cause instability (GHZ_L = loop-gain = $1 \angle 180^\circ$). The plot of this critical load versus frequency is then compared with a plot of the motor load as a function of frequency (see Figure 21).

From a comparison of the two plots, it can be determined whether this particular motor load can cause instability. A more thorough dissertation of this testing method and stability criteria is given in Chapter VI. As a method of insuring the stable operation of amplifier/motor combinations, this method is not feasible. A large amount of time and effort is required to obtain the frequency characteristics of each individual amplifier. However, this method of obtaining the open-loop gain characteristics is valuable and necessary to determine a worst-case dummy load which can be used to test amplifiers. It is also useful in

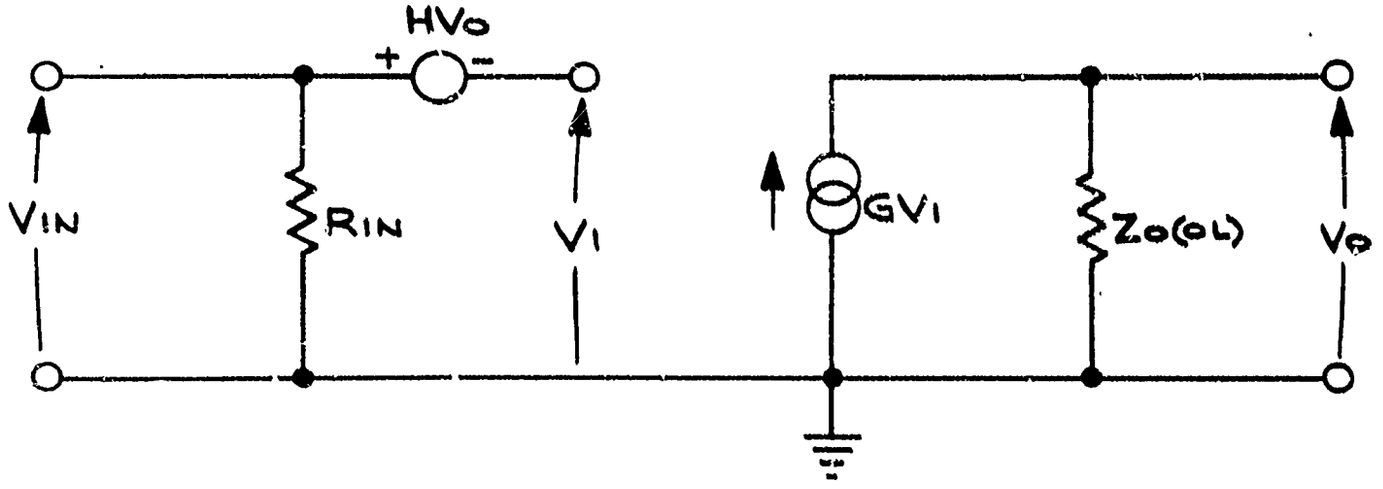

FIG 2 SERVO AMPLIFIER EQUIVALENT CIRCUIT

the design of servo amplifiers. From the standpoint of specifications, this method would require the specification of limits for open-loop gain characteristics which would be difficult to check in the incoming qualification of amplifiers.

The method suggested for specifying and testing production amplifiers and motors for compatibility is called the worst-case stability dummy load test method. Either by means of previous experience or by means of obtaining the open-loop characteristics of a sample of amplifiers, the general open-loop gain characteristics of the amplifiers must be known. With this knowledge, a proper selection of servomotor parameters can be made which will result in a worst-case stability dummy load. This load is effectively the worst load with respect to stability to which the amplifier may be subjected. Each amplifier may be tested with this specified dummy load to insure stable operation with a specific size of motor over an entire frequency range. The only necessary addition to present amplifier specifications is to include testing the amplifier with the worst-case dummy load.

In order to properly determine a dummy load which will simulate the servomotor characteristics over the frequency range of interest, a more thorough servomotor specification is necessary. The additional specifications required include a tolerance on R_s and X_{LS}, the DC resistance (R_{DC}) with an appropriate tolerance, and the maximum value of the leakage inductance (L_{LP}). Justification for the addition of these parameters lies in the requirement for a more accurate motor model. Chapters V and VII and NAFI TR-1053 validate the necessity of an improved motor model.

Economically speaking, the dummy load method of testing with the addition of these few parameters is the best approach. The justification for the increase in price for the addition of these specifications of course reverts back to the savings that will result due to reductions of production shut-downs caused by the stability problem. Normally, when the stability problem occurs, an analysis of the problem results which can also add an appreciable amount to the already high cost of the shut-down.

V. SERVOMOTOR DISCUSSION

A. SERVOMOTOR DESCRIPTION

1. Equivalent Circuits

Servomotor manufacturers' specifications list the equivalent series circuit parameters as shown in the equivalent series motor model of Figure 3.

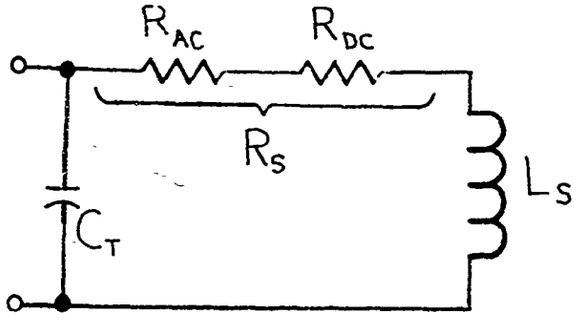

Figure 3 Equivalent Series Motor Model

The inability of this series circuit to properly simulate actual motor impedance over the frequency range of interest necessitates the use of a more complex servomotor equivalent circuit. Most literature uses the simplified equivalent circuit shown in Figure 4 to represent one phase of a servomotor operating under balanced conditions. However, servomotors with center-tapped control winding for push-pull amplifier applications suggest an equivalent circuit with three input terminals. Actual servo amplifier operation as shown in Figure 1 further justifies this idea. Therefore, Figure 5, the modified servomotor equivalent circuit as suggested in NAFI TR-1053, is the choice for most practical applications with balanced input motor voltages. In a null-type servo system, the voltage on the control phase will be much less

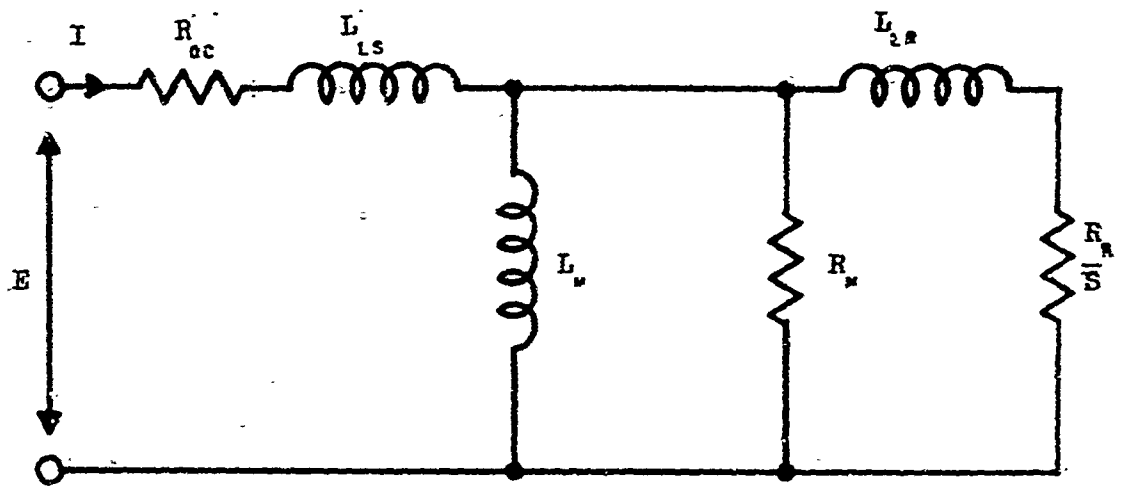

Figure 4 Complex Equivalent Circuit of the Servomotor

SYMBOL = SERVOMOTOR PARAMETER

R_{DC} = Stator copper loss

L_{LS} = Stator leakage inductance

L_{LR} = Rotor leakage inductance

L_M = Magnetizing inductance

R_M = Core loss

R_R = Rotor resistance

S = Slip

$\frac{R_R}{S}$ = Effective rotor resistance

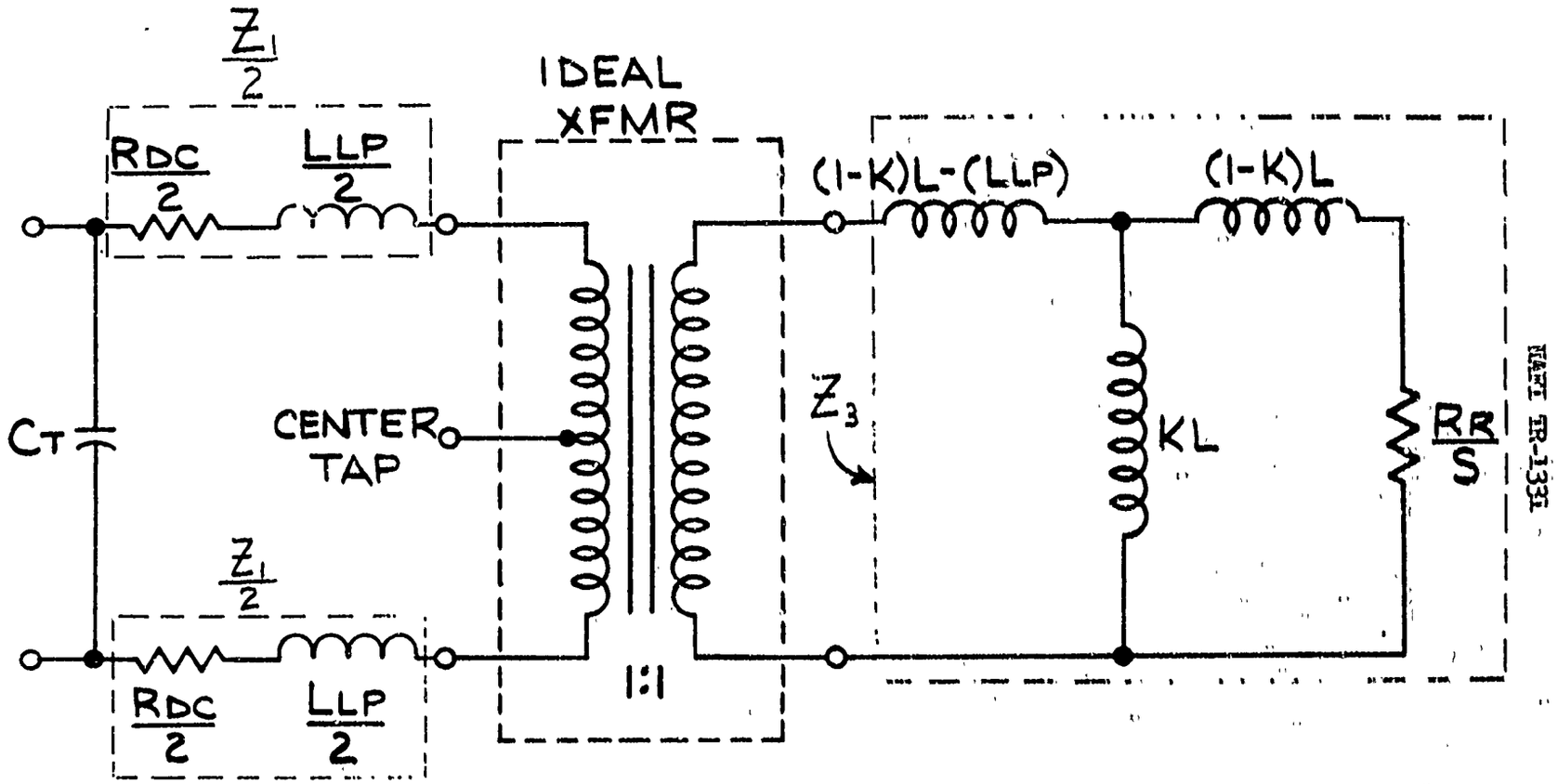

FIG. 5 IDEAL DUMMY LOAD FOR THE COMPLEX MOTOR MODEL

than the rated value a large percentage of the time. However, an analysis of the loads for an unbalanced and a balanced case, using the CODED circuit analysis computer program, resulted in little significant difference between the loads at frequencies away from 400 Hz.

2. Equivalent Circuit with Center-Tap Control Winding

In Figure 5, the control phase winding DC resistance (R_{DC}) and the leakage inductance (L_{LP}) between the halves of the control winding are shown in the primary circuit of an ideal transformer. This transformer is necessary to reflect the load to either half of the control winding depending on which half of the amplifier output is operating. The symmetric transformer equivalent simulates the stator and rotor loading in the secondary as follows: The magnetizing inductance and the stator and rotor leakage inductances are represented in terms of the coupling coefficient (K) between stator and rotor windings. R_R/S is the effective resistance of the rotor. Note that the iron magnetization losses represented by resistance R_M in Figure 4 are ignored. According to most sources, this is a fair approximation since the ratio of R_M to X_{LM} is much greater than one. The impedance groups of Za and Zb are utilized in the procedure to determine the equivalent circuit parameters.

B. EQUIVALENT SERIES CIRCUIT PARAMETER CORRELATION

In order to specify worst-case dummy loads, the servomotor parameters must have limits associated with each of them. Initially, the motor parameter limits were established and a dummy load developed, based on the assumption that all motor parameters were independent of each other. However, nearly every amplifier tested with this load exhibited unstable operation. After further investigation, it was determined that there is correlation between the R_{DC}, R_S, and X_{LS} motor parameters, and this was not considered in the initial dummy load. The result was that the dummy load parameters were placed at their uncorrelated extremes in such a way that actual motor parameter data would not come close to the dummy load data. For example, consider the plot of R_S versus X_{LS} for several motor samples as illustrated in Figure 6. It was determined that the condition where X_{LS} is maximum and R_S is minimum is the worst case as far as stability is concerned. The uncorrelated parameter specifications would have indicated the use of data corresponding

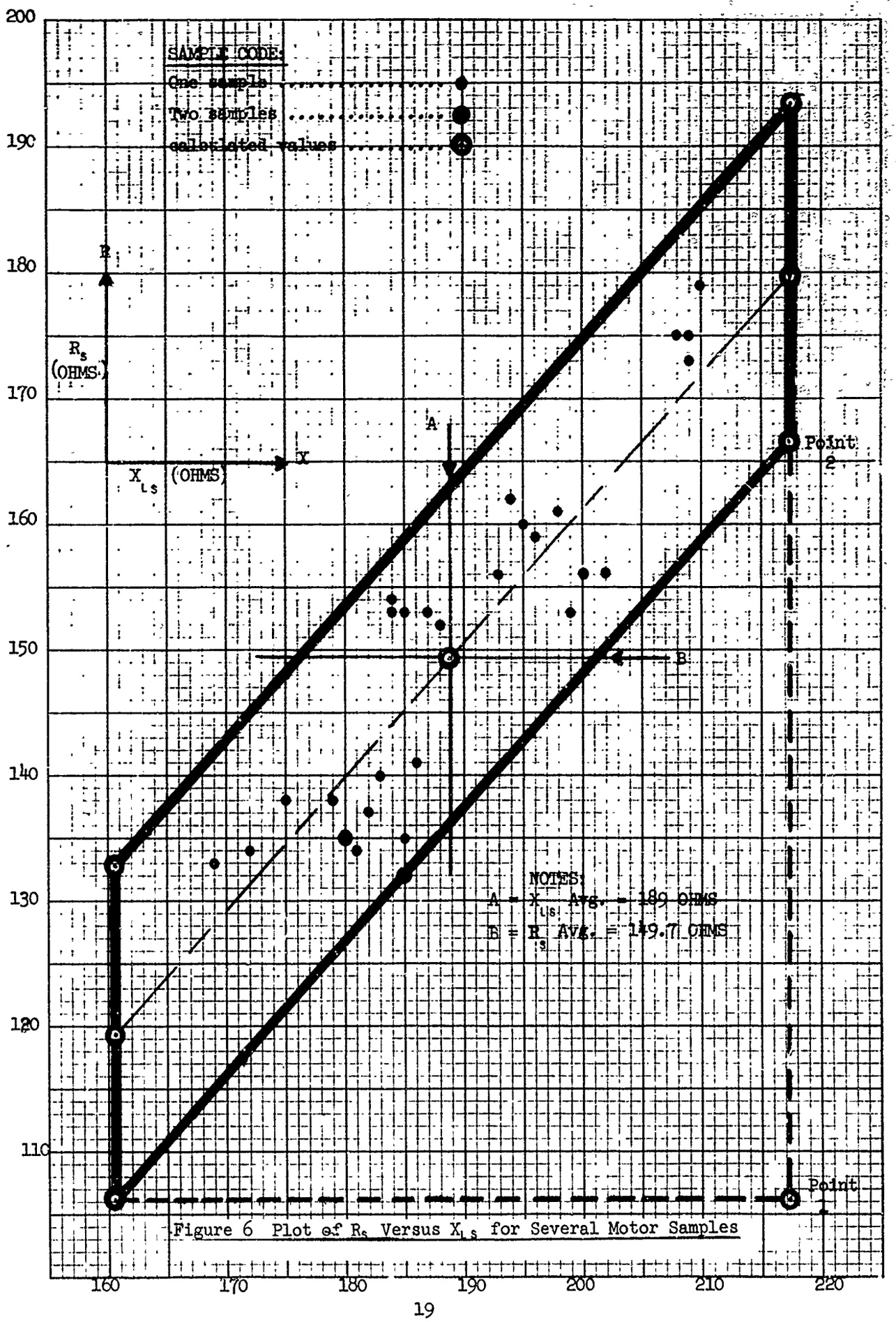

Figure 6 Plot of R_s Versus X_{Ls} for Several Motor Samples

to point 1 (Figure 6) while all of the data fell within the parallelogram indicated by the heavy lines. Actually, the data at point 2 represents a much more realistic worst-case set of data for dummy load determination.

The simple series equivalent circuit of the servomotor was used because a large part of the experimental data available for this study consisted of data for the simple case only. Most of the actual motors were not available for further testing, so all data correlation and distribution information had to be derived from the series equivalent circuit. The servomotors for which data was available are listed in Table III. Table IV lists the series equivalent circuit parameters received from Kearfott and NAD, Crane, Indiana. Table V gives the series equivalent circuit parameters and the complex equivalent circuit parameters for the servomotors tested at NAFI. As it will be pointed out later, the worst-case dummy load was first determined in terms of the series circuit parameters and then converted to the more complicated equivalent circuit (Figure 5) for experimental testing.

Excluding temperature variations, the DC resistance (R_{DC}) in properly wound motors is dependent only upon type, size, and length of the control winding wire. However, actual sample tests on 30 motors revealed worst-case variations of +45% and -30% from the sample average. The value of tuning capacitor (C) is determined by the value of the inductive reactance (X_{LS}) at the design carrier frequency. The variation in value of the leakage inductance (L_{LP}) is mostly due to internal design and manufacturing process. In contrast to the smallness of L_{LP} and its control, L_S is much larger and more controllable. In fact, laboratory tests on motors with consecutive serial numbers from a given manufacturer generally have less than ten per cent variations in X_{LS}. Many have variations of less than one per cent. Laboratory tests on sizes 8, 11, and 15 motors from seven manufacturers revealed that each of the approximately 30 motors per size exhibited an X_{LS} value within ± 15% of their respective sample average. However, the same tests indicated that the R_{DC} value fell within the range of -30% to +46% of the sample average. At the same time, the worst-case values of R_S had a 72% (of sample average) spread.

TABLE III Servomotors

NOTE: THE NUMERICAL PART OF THE IDENTIFICATION CODE DESIGNATES THE MOTOR SIZE.

IDENTIFICATION CODE	MANUFACTURER	MODEL NO.	SERIAL NO.
8A	KEARFOTT	2474474	Y
8B	"	"	Z
8C	VERNITRON	8SM4-12R	2
8D	KEARFOTT	2474474	1
8E	"	"	2
8F	"	"	3
8G	"	"	4
8H	"	"	5
8I	"	"	6
8J	"	"	7
8K	"	"	8
8L	MCMASTERS	26V-08SM4a	00005
8M	"	"	00001
8N	"	"	00002
8P	"	"	00004
8Q	WESTON-TRANS.	"	3421-1
8R	"	"	3421-2
8S	"	"	3421-3
8T	"	"	3421-4
8U	VERNITRON	"	1X
8V	"	"	2X
8W	"	"	3X
8X	"	"	4X
8Y	IMC	"	1
8Z	"	"	2
8AA	"	"	3
8BB	"	"	4
8CC	HAROWE	"	5
8DD	"	"	6
8EE	"	"	9
8FF	"	"	10
11A	KEARFOTT	2474475	A
11B	"	"	B
11C	"	"	C
11D	TACHTRONIC	"	105
11E	"	"	106
11F	"	"	107
11G	KEARFOTT	2474475	1
11H	"	"	2
11I	"	"	3
11J	"	"	4
11K	"	"	5
11L	"	"	6
11M	"	"	7

TABLE III Servomotors (continued)

IDENTIFICATION	MANUFACTURER	MODEL NO.	SERIAL NO.
11N	KEARFOTT	2474475	8
11P	MCMASTERS	11SM4C	00001
11Q	"	"	00002
11R	"	"	00003
11S	"	"	00005
11T	WESTON-TRANS.	"	3421-7
11U	"	"	3421-8
11V	"	"	3421-9
11W	"	"	3421-10
11X	IMC	"	1
11Y	"	"	2
11Z	"	"	3
11AA	"	"	4
15A	KEARFOTT	2474476	7
15B	"	"	8
15C	TACHTRONIC	"	102
15D	"	"	103
15E	KEARFOTT	247447	1
15F	"	"	2
15G	"	"	3
15H	"	"	4
15I	"	"	5
15J	"	"	6
15K	"	"	7
15L	"	"	8
15M	HAROWE	15SM4d	17
15N	"	"	18
15P	"	"	20
15Q	"	"	21
15R	WESTON-TRANS.	"	3421-13
15S	"	"	3421-14
15T	"	"	3421-15
15U	"	"	3421-16
15V	IMC	"	1
15W	"	"	2
15X	"	"	3
15Y	"	"	4

TABLE IV Servomotor Equivalent Series Circuit Parameters Obtained from Kearfott* and NAD**, Crane, Indiana

IDENTIFICATION CODE	X_{ls} (OHMS)	R_s (OHMS)	R_{DC} (OHMS)	R_{AC} (OHMS)
8D	179.3	138.1	79.9	58.2
8E	180.0	135.0	79.5	55.5
8F	202.2	155.7	85.8	69.9
8G	182.2	136.7	79.3	57.4
8H	184.8	135.3	79.3	56.0
8I	185.2	132.1	78.8	53.3
8J	185.2	132.1	77.1	55.0
8K	180.0	135.0	79.6	55.4
8L	193.8	161.8	87.6	74.2
8M	195.6	159.2	89.4	69.8
8N	198.4	160.5	89.4	71.1
8P	198.7	153.2	88.8	64.4
8Q	184.0	153.5	98.6	54.9
8R	174.5	148.2	101.5	46.7
8S	195.2	160.3	98.0	62.3
8T	193.4	156.0	97.0	59.0
8U	209.1	175.0	102.0	73.0
8V	209.3	172.5	101.4	71.1
8W	208.2	174.6	103.5	71.1
8X	210.4	179.2	102.5	76.7
8Y	168.6	133.3	85.0	48.3
8Z	180.5	134.4	84.5	49.9
8AA	174.7	138.4	85.2	53.2
8BB	172.2	133.5	84.0	49.5
8CC	184.1	152.8	91.0	61.8
8DD	187.1	152.9	90.4	62.5
8EE	187.8	152.0	91.9	60.1
8FF	184.6	153.3	91.9	61.4
11G	175.0	103.7	26.8	76.9
11H	181.0	110.1	26.4	83.7
11I	175.0	103.7	24.7	79.0
11J	170.9	104.0	27.0	77.0
11K	173.2	111.1	27.5	83.6
11L	173.7	105.8	26.6	79.2
11M	172.2	110.4	27.0	83.4
11N	170.9	104.0	27.6	76.4
11P	183.2	112.6	28.5	84.1
11Q	179.4	109.0	28.2	80.8
11R	171.3	97.9	28.4	69.5
11S	175.7	99.0	28.5	70.5
11T	183.1	148.0	37.7	110.3
11U	184.4	149.9	37.7	112.2
11V	186.0	158.7	37.2	121.5

TABLE IV (Continued)

IDENTIFICATION CODE	X_{L_S} (OHMS)	R_S (OHMS)	R_{D_C} (OHMS)	R_{A_C} (OHMS)
11W	186.5	157.2	37.6	119.6
11X	202.3	165.5	43.8	121.7
11Y	204.5	164.3	43.4	120.9
11Z	199.2	162.3	43.0	119.3
11AA	189.4	174.6	44.5	130.1
15E	88.3	53.5	11.2	42.3
15F	89.4	51.5	11.2	40.3
15G	89.1	51.5	11.2	40.3
15H	91.3	50.1	11.3	38.8
15I	90.3	52.2	11.2	41.0
15J	89.1	51.5	11.1	40.4
15K	90.4	52.2	11.2	41.0
15L	88.9	54.2	11.2	43.0
15M	96.7	58.2	12.3	45.9
15N	93.0	60.0	12.4	47.6
15P	95.1	59.7	12.5	47.2
15Q	95.5	61.6	12.4	49.2
15R	97.0	60.2	11.0	49.2
15S	96.7	61.1	10.9	50.2
15T	97.9	62.8	10.9	51.9
15U	97.8	62.6	11.1	51.5
15V	106.4	71.9	16.0	55.9
15W	105.1	70.4	16.4	54.0
15X	104.6	74.6	17.0	57.6
15Y	106.2	72.0	16.3	55.7

* Bureau of Naval Weapons Contract Number NOW 62-1000-F awarded to Kearfott Division, General Precision, Inc., Little Falls, New Jersey.

** Naval Ammunition Depot

TABLE V

SERVOMOTOR EQUIVALENT CIRCUIT PARAMETERS FOR MOTORS TESTED AT NAFI

ID CODE	SERIES EQUIVALENT CIRCUIT				COMPLEX EQUIVALENT CIRCUIT				
	R_{oc} (OHMS)	R_{Ac} (OHMS)	R_s (OHMS)	X_{Ls} (OHMS)	$R1(R_{oc})$ (OHMS)	L_{Lp} (mh)	K	L (mh)	R_2 (OHMS)
8A	88	52.3	140.3	182.8	88	1.84	.737	84.5	385
8B	88	67.5	155.5	199.7	88	1.72	.730	87.7	380
8C	86.4	54.1	138.1	186.1	86.4	1.78	.795	85.6	300
11A	28.9	55.6	84.5	168.6	28.9	1.59	.815	83.2	387
11B	28.7	68.2	96.9	171	28.7	1.71	.83	88.4	250
11C	29.3	62	91.3	163.7	29.3	1.59	.823	83.6	310
11D	35.7	76.9	112.6	166.2	35.7	.9	.884	96.6	355
11E	35.7	84.8	120.5	164.2	35.7	.96	.875	92.0	320
11F	36	70.4	106.4	164.5	36.0	.97	.859	89.8	310
15A	12.73	36.77	49.5	91.5	12.73	1.04	.8	44.75	184
15B	12.06	32.64	44.7	91.1	12.33	.84	.779	43.8	185
15C	16.08	53.82	69.9	109.9	16.08	.61	.859	68.8	192
15D	16	54.7	7[illegible]7	104.8	16.00	.58	.885	66.75	198

It can be seen from the above parameter spreads, that the parameter most closely controlled and most easily specified is X_{LS}. It was for this reason that X_{LS} was chosen as the independent variable in a correlation analysis of the motor parameters. All of the sample values of R_S and R_{DC} were plotted versus X_{LS} as illustrated in Figures 6 and 7 for size 8 motors. The linear least squares fit relationships between each of the sets of data were determined using a library computer program provided by the G.E. time-sharing service. A ± 15% tolerance around the sample average was placed on the value of X_{LS} since all of the data fell within this range. Lines were then drawn parallel to the best linear fit line and displaced from this line by an amount equal to ± 15% of the R_S and R_{DC} sample averages. The resulting parallelogram specifies a much more realistic region in which the sets of parameters of "acceptable" motors must lie. If a motor data set lies outside this region, the stability predicted by the worst-case dummy load cannot be guaranteed. At least 90% of all motors tested for this study fell within the regions specified.

It can be seen that there now exists two values for each of the extremes of R_S and R_{DC} corresponding to the maximum and minimum values of X_{LS}. The sets of data corresponding to the corners of the parallelograms will be used as the parameter extremes necessary for worst-case dummy load determinations.

Figure 8 illustrates a matrix of all the possible worst-case loads.

C. COMPLEX EQUIVALENT CIRCUIT PARAMETER DETERMINATION

1. From Experimental Test Results:

Using measurement techniques as given in NAFI TR-1053, Z_0, Z_S, and Z_A of the control winding must be measured at various frequencies along the band of interest. These impedances are given in Figure 9 along with their definition in terms of motor impedances Z_1 and Z_3 as previously shown in Figure 5. The values of Z_1 and Z_3 are then calculated for each frequency with the aid of a time-sharing computer program given in Figure 10. A print-out of the results of one of these calculations is given in Figure 11. Note that the print-out provides a check of the data by supplying the measured and calculated values of Z_1 for comparison.

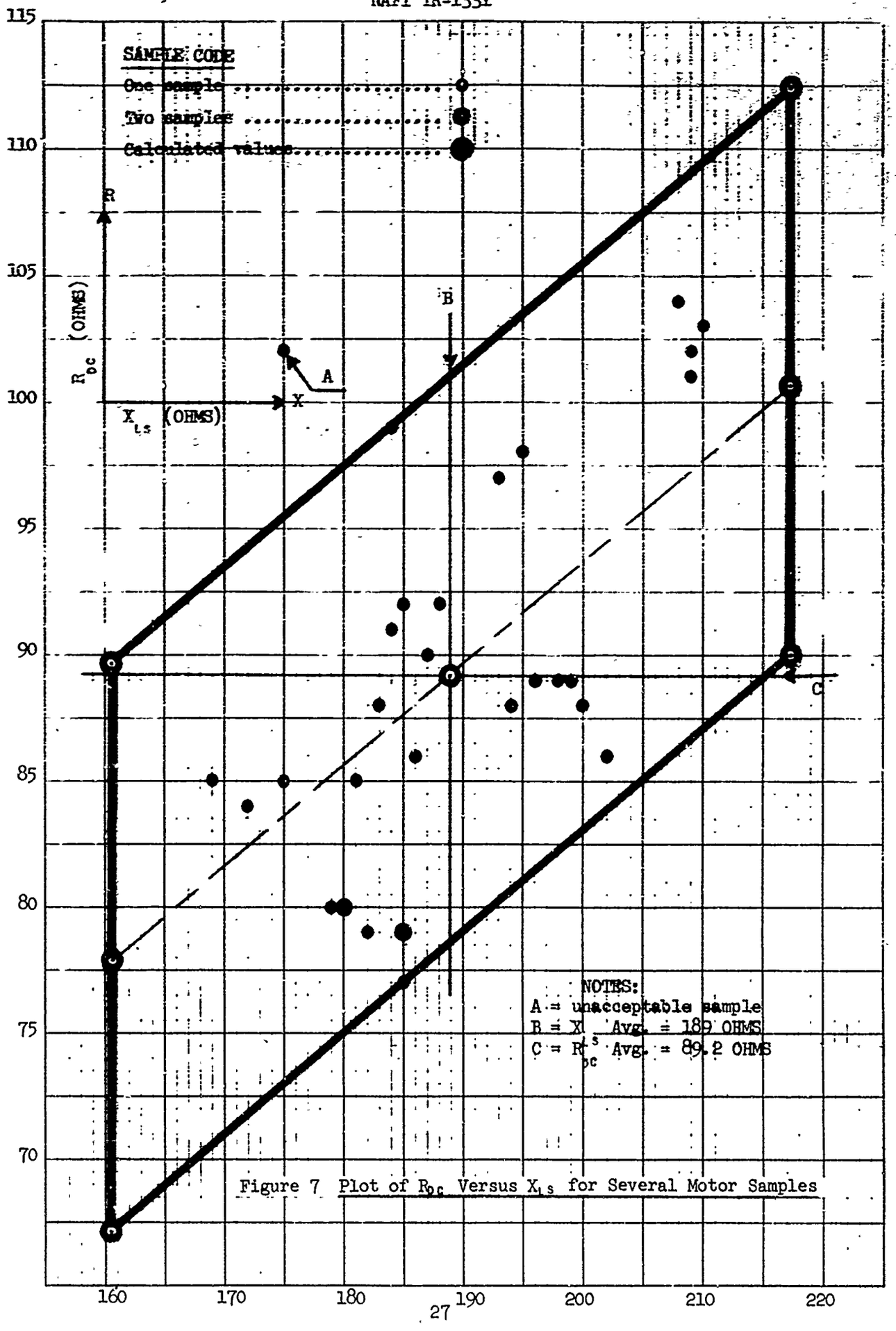

Figure 7 Plot of R_{DC} Versus X_{LS} for Several Motor Samples

	R_{DC} (MAXIMUM)		R_{DC} (MINIMUM)		
X_{LS} (MAX.)	60*	61	51	50	R_S (MAX.)
X_{LS} (MIN.)	30	31	41	40	R_S (MAX.)
	20	21	11	10	R_S (MIN.)
X_{LS} (MAX.)	70	71	81	80	R_S (MIN.)
	C_T (MIN.)	C_T (MAX.)		C_T (MIN.)	

Figure 8 Matrix of Possible Combinations of Extreme Motor Parameters

*These numbers represent a code for each particular combination of parameters.

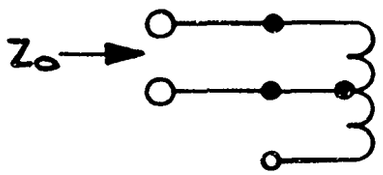

$$Z_o = \frac{1}{2}\left(Z_1 + \frac{Z_3}{2}\right)$$

A. OPEN CIRCUIT

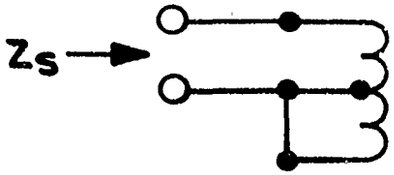

$$Z_s = Z_1 \frac{(Z_1 + Z_3)}{2Z_1 + Z_3}$$

B. SHORT CIRCUIT

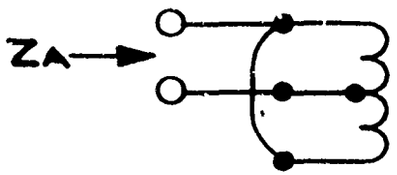

$$Z_A = \frac{Z_1}{4}$$

C. ANTIPARALLEL

$$Z_1 = 4Z_A = 2\left[Z_o - \sqrt{Z_o(Z_o - Z_s)}\right]$$

$$Z_3 = 4\sqrt{Z_o(Z_o - Z_s)}$$

$$Z_o \cdot Z_s = 4Z_A(Z_o - Z_A)$$

FIG.9 SERVOMOTOR IMPEDANCE DETERMINATION
(AS SUGGESTED IN NAFI TR-1053)

```
10 REM INSERT DATA IN LINES 1000 TO 2000. THE ORDER OF DATA IS-
20 REM FREQUENCY, V0, VIO, THETA, VS, VIS, PHI, VA, VIA, ALPHA.
100 PRINT "CALCULATION OF SERVO MOTOR IMPEDANCE Z1 AND Z3."
110 PRINT
120PRINT"ENTER NO. OF FREQUENCIES AND VALUE OF CURRENT SENSING RESISTOR"
130 INPUT N,R1
140 DIM F(15)
150 DIM O(15)
160 DIM S(15)
180 DIM D(15)
190 DIM E(15)
202 PRINT
204 LET K=1
206 PRINT "FREQ","Z1 MAG (MEAS)","Z1 ANG (MEAS)"
210 READ C,V0,V1,A1,V2,V3,A3,V4,V5,A5
220 LET F(K)=C
230 LET O(K)=V0*R1/V1
240 LET S(K)=V2*R1/V3
260 LET D(K)=A1/57.296
270 LET E(K)=A3/57.296
280 PRINT F(K),4*V4*R1/V5,A5
290 LET K=K+1
300 IF K<=N THEN 210
310 PRINT
320 PRINT"FREQ","Z3 MAG","Z3 ANG","Z1 MAG (CAL)","Z1 ANG (CAL)"
330 LET K=1
340 LET Z1=O(K)*COS(D(K))
350 LET Z2=O(K)*SIN(D(K))
360 LET Z3=S(K)*COS(E(K))
370 LET Z4=S(K)*SIN(E(K))
380 LET Z5=SQR((Z1-Z3)↑2+(Z2-Z4)↑2)
390 LET T5=ATN((Z2-Z4)/(Z1-Z3))
400 IF (Z1-Z3)<0 THEN 420
410 GO TO 460
420 IF(Z2-Z4)>=0 THEN 450
430 LET T5=-3.1416+T5
440 GO TO 460
450 LET T5=3.1416+T5
460LET Z6=SQR(O(K)*Z5)
470 LET T7=((D(K)+T5)/2)*57.296
480 LET Z7=4*Z6
490 LET Z8=Z6*COS(T7/57.296)
500 LET Z9=Z6*SIN(T7/57.296)
530 LET  X3=2*SQR((Z1-Z8)↑2+(Z2-Z9)↑2)
540 LET T3=ATN((Z2-Z9)/(Z1-Z8))*57.296
550 PRINT F(K),Z7,T7,X3,T3
560 LET K=K+1
570 IF K<=N THEN 340
575 PRINT
580 PRINT" IF MORE DATA NEEDS TO BE PROCESSED, TYPE IN NEW DATA AND"
581 PRINT "RUN AGAIN"
1000 DATA 0
9999 END
```

Figure 10 Time-Sharing Computer Program for Calculation of Motor Impedances Z_1 and Z_3

```
S-MOTO     15:52    CH-E WE 10/11/7

CALCULATIØN ØF SERVØ MØTØR IMPEDANCE Z1 AND Z3.

ENTER NØ. ØF FREQUENCIES AND VALUE ØF CURRENT SENSING RESISTØR
? 12,50.25

 FREQ          Z1 MAG [MEAS]   Z1 ANG [MEAS]
  40             28.8938          3.6
  100            28.8938          5.7
  200            30.15            10.4
  300            30.9038          15.3
  400            32.16            18.3
  500            34.17            21.7
  600            35.6775          24.2
  1000           40.7025          31.1
  4000           80.4             50.7
  10000          145.725          59.7
  40000          389.438          69.1
  100000         854.25           77.2

 FREQ          Z3 MAG          Z3 ANG          Z1 MAG [CAL]    Z1 ANG [CAL]
  40             17.9421          42.1675         23.369          11.2639
  100            48.7088          82.1075         28.7323         4.48266
  200            104.209          78.025          29.4477         10.8801
  300            136.673          73.0499         31.661          14.8957
  400            167.455          71.2285         32.6309         18.7388
  500            200.744          69.6922         33.6832         22.2425
  600            227.975          68.5288         34.8347         23.2682
  1000           326.425          67.2633         39.8336         28.8
  4000           882.042          64.9246         88.9767         50.3961
  10000          1856.85          69.271          141.125         59.6089
  40000          7073.07          69.7973         383.025         70.8487
  100000         19702.6          -42.7853        812.296         79.1365

 IF MØRE DATA NEEDS TØ BE PRØCESSED, TYPE IN NEW DATA AND
RUN AGAIN

TIME:   5 SECS.
```

Figure 11 Calculated Values of Motor Impedances Z_1 and Z_3

The equivalent circuit parameter values of Figure 5 are calculated from the Z_1 and Z_3 magnitude and angle versus frequency plots shown in Figure 12. From these plots, the significant break frequencies and asymptotic values are obtained. Then, using the equations in Figure 12, the equivalent circuit values are determined.

2. From Mathematical Manipulation of Equivalent Series Circuit Parameters:

Extreme parameter values have been determined for the series equivalent circuit, but the complex equivalent circuit more accurately represents actual motor impedances over the frequency range of interest. To determine which of the 16 possible dummy load configurations (see Figure 8) represents the worst-case stability load, the complex equivalent circuit should be determined and evaluated for each of the 16 possible loads. Areas of probable instability occur at frequencies other than 400 Hz; therefore, the complex circuit is necessary. A comparison of the frequency responses of the two different equivalent circuits is presented in Figure 25b, page 61.

Figure 13 illustrates the two circuits which must be equated at 400 Hz to arrive at parameter values for the complex equivalent circuit. The variables which must be determined are K, L, and R, and the necessary equations are also given in Figure 13. After a value of K is assumed, equation (1) is solved to determine a value of L which is used in equation (2). These equations are solved using a time-sharing computer library program. These equations must be solved several times for different values of K until an acceptable value of K is determined. The preferred values of K (0.6 to 0.9) and R are those close to values obtained on the few motors tested in the lab. In some cases, two values of R are obtained in the allowable range, and the lower value of R is chosen since it is closer to the experimental values obtained.

The results for the servomotors tested at NAFI are given in Table V, page 25.

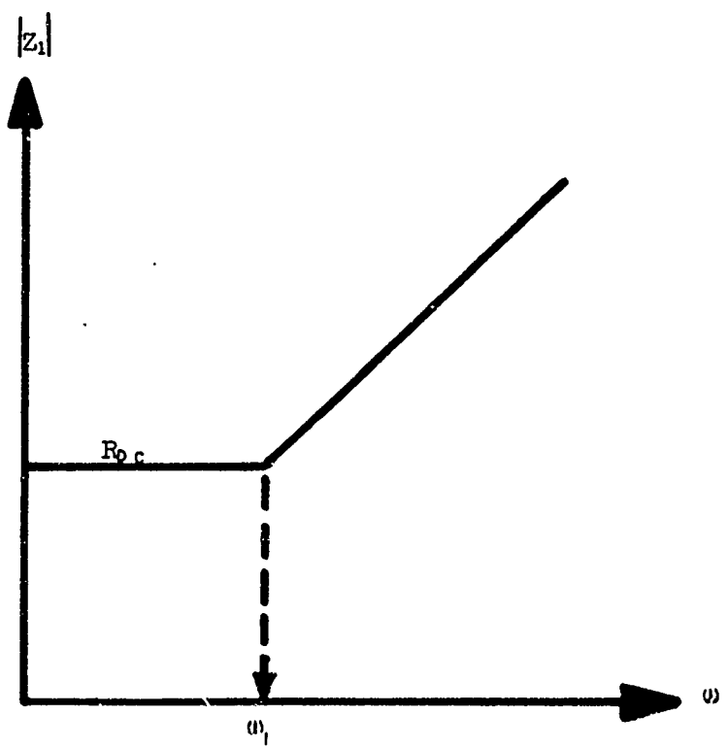

(1) $L_{LP} = R_{DC}/\omega_1$

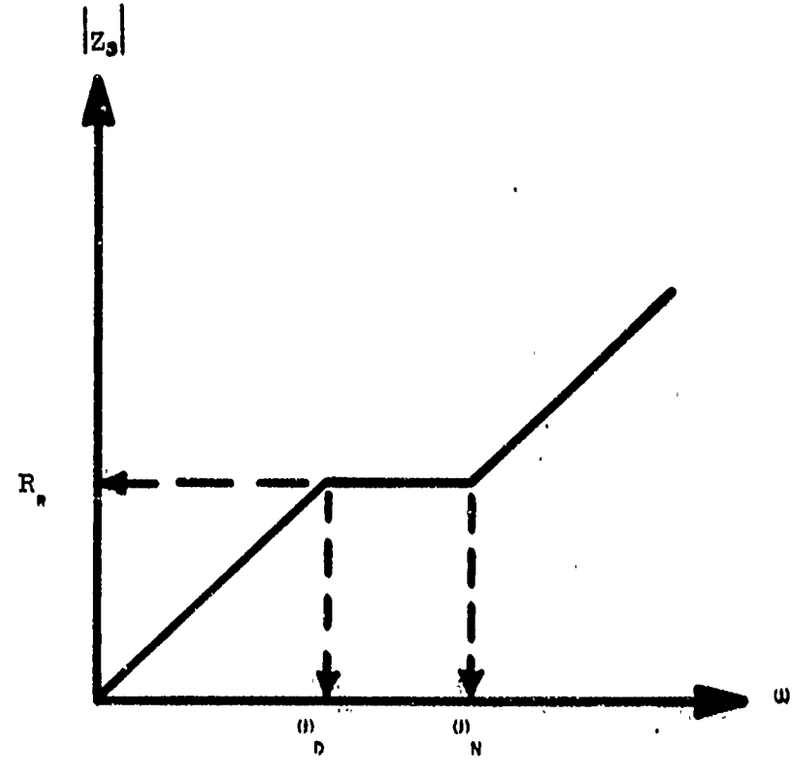

(2) $K = (1 - \omega_D/\omega_N)^{\frac{1}{2}}$

(3) $L = R_R/\omega_D$

Figure 12 · Bode Plots of $|Z_2|$ and $|Z_3|$

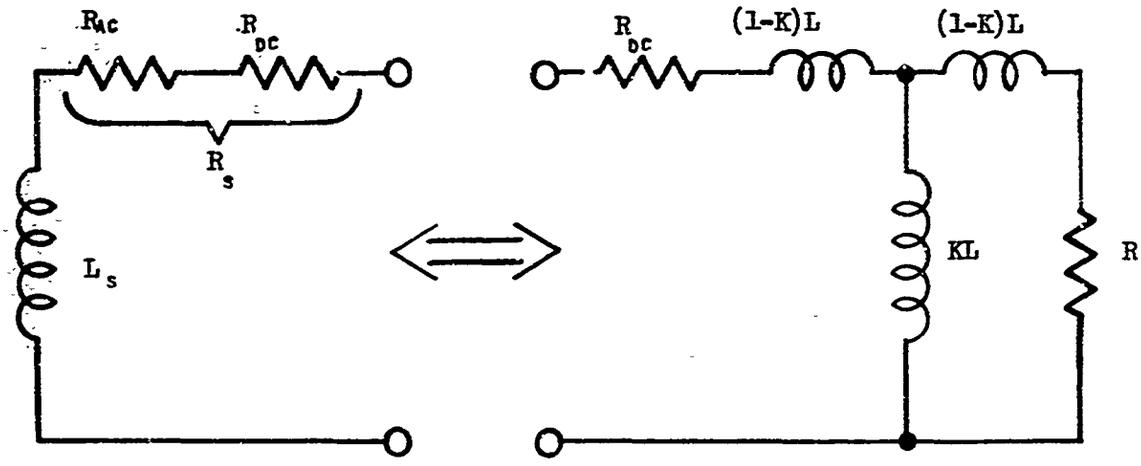

a. Equivalent Series b. Symmetric Transform Equivalent

EQUATION RESULTS:

$$(1)\quad L^2 = \frac{R^2}{\omega\left[\frac{K^2 R}{R_s - R_{DC}} - 1\right]}$$

$$(2)\quad R^2 - \frac{R^2 \omega L}{X_{LS}} + \omega^2 L^2 - \frac{(1-K^2)}{X_{LS}}\,\omega^3 L^3 = 0$$

Figure 13 Equivalent Servomotor Circuits

A minimum possible value of K can be calculated from the following equation:

$$K_{min} = \frac{1}{Q_x} \sqrt{2(\sqrt{1 + Q_x^2} - 1)} \qquad (5\text{-}1)$$

where $Q_x = \frac{2\pi f L_s}{R_s - R_{oc}}$

The actual value of K chosen has a secondary effect on the motor transfer impedance, Z_{12}, and consequently, on stability as can be seen in Figure 25b, page 61.

VI. SERVO AMPLIFIER DISCUSSION

A. GENERAL DESCRIPTION

The individual representation of motor impedances Z_{11} and Z_{12} constitute the motor portion of the servo amplifier/servomotor flow graph shown in Figure 1. The remainder of the flow graph depicts internal amplifier operation. The following equations give the closed loop gain of each half of the amplifier:

$$\frac{V_{0A}}{V_{IN}} = \frac{G_2 G_{3A} G_{MA} Z_{11}}{1 - G_2 G_{3A} G_{MA} Z_{12} H_1} \qquad (6\text{-}1)$$

$$\frac{V_{0B}}{V_{IN}} = \frac{G_2 G_{3B} G_{MB} Z_{11}}{1 - G_2 G_{3B} G_{MB} Z_{11} H_1} \qquad (6\text{-}2)$$

From these gain equations, the system characteristic equations are:

$$G_2 G_{3A} G_{MA} Z_{12} H_1 - 1 = 0 \qquad (6\text{-}3)$$

$$G_2 G_{3B} G_{MB} Z_{11} H_1 - 1 = 0 \qquad (6\text{-}4)$$

The amplifier/motor combination will oscillate if either equation 6-3 or 6-4 is satisfied. It is obvious that the GH of the amplifier ($G_1 G_2 G_3 G_M H_1$) is necessary for loop gain calculations. Usually, none of these internal parameter values are available, and it is, therefore, necessary to obtain them by measurements.

In Chapter IV it is pointed out that obtaining the loop gain characteristics by means of CODED analysis or by open-loop frequency

response testing is not feasible in a production environment. Therefore, it is necessary to develop a technique employing external measurement with no access to the feedback loop to determine the internal part of the loop gain.

B. GH OBTAINED BY EXTERNAL MEASUREMENT

1. Equation to Demonstrate Feasibility

It is relatively easy to show how GH may be measured if the circuit has only a single feedback loop. Figure 14 illustrates the flow graph diagram representation of both the closed loop transfer function (C/R) and the impedance measured at the output terminals (Z_M) with a load impedance Z_L attached. Z_M can be obtained by driving the output terminals with an external current source (I_{0x}) and measuring the resulting voltage. The amplifier input terminals are shunted with a resistance equal to that value used as the amplifier source resistance in the servo system.

In the equation for Z_M, everything except the GH product is known. Figures 15 and 16 illustrate that the same GH measuring technique may also be applied to amplifiers which have multiple or internal feedback loops.

2. Measurement Techniques

The GH measurement method consists of obtaining the output impedance of the feedback side of the amplifier over the frequency range of interest. (40 Hz to 100 KHz was used for the laboratory measurements phase of this project.) The circuit utilized is illustrated in Figure 17.

At discrete frequencies in the range of interest, the value of R_L and the data to compute Z_M are entered into a computer program to compute GH and the load Z_L which will make $GHZ_L = 1\underline{/180°}$. This load shall be called Z_L (unstable). The computer program flow chart is illustrated in Figure 18. Figure 19 presents the computer program as written in G.E. card fortran and Figure 20 presents the computer program as written in time-sharing basic language.

Table VI presents the names of the variables used in these computer programs.

3. GH for Non-Feedback Side of the Amplifier

The GH calculated from the output impedance measurements is only for the feedback side of the amplifier (see Figure 1). For the non-feedback side of the amplifier, the absolute value of GH is approximately the same and the phase is 180° from the phase of the feedback side. The value of GH for the non-feedback side cannot be measured by external means.

C. HOW TO OBTAIN Z_{11} AND Z_{12} (unstable) CURVES FROM GH CURVES

Since the magnitude of GH is assumed equal for both sides of the amplifier, the magnitude of Z_{11} or Z_{12} (for borderline stability) would

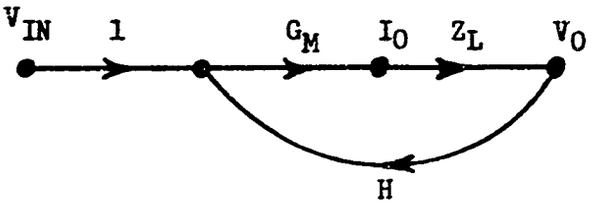

$$\frac{C}{R} = \frac{V_O}{V_{IN}} = \frac{G_M Z_L}{1 - G_M Z_L H}$$

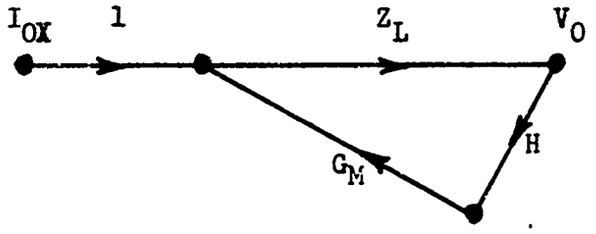

$$Z_M = \frac{V_O}{I_{OX}} = \frac{Z_L}{1 - G_M Z_L H}$$

Figure 14 Flow Diagrams of a Single Loop Amplifier

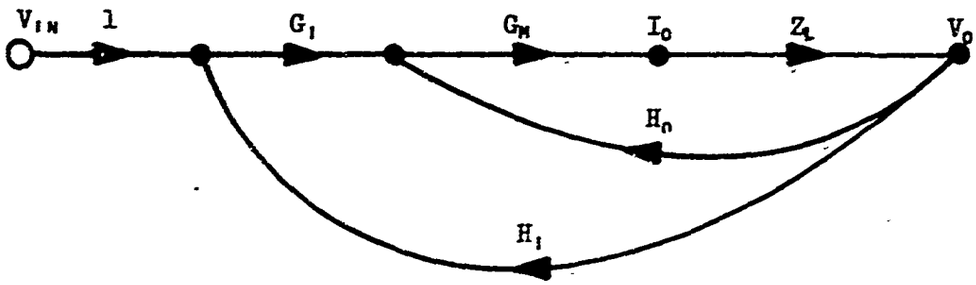

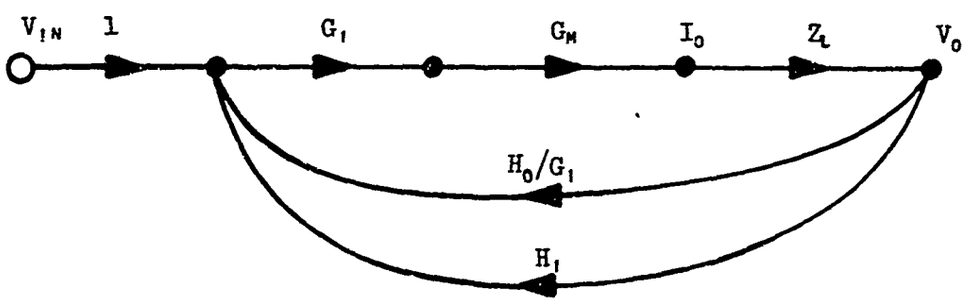

$$\frac{C}{R} = \frac{V_O}{V_{IN}} = \frac{G_I\, G_M\, Z_L}{1 - G_I\, G_M\, Z_L \left(H_I + \dfrac{H_O}{G_I} \right)}$$

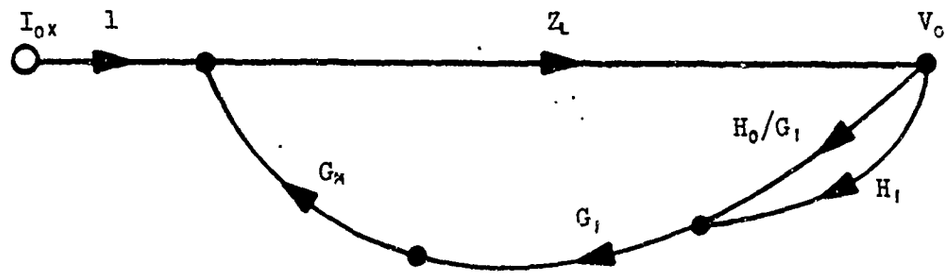

$$Z_M = \left. \frac{V_O}{I_{OX}} \right|_{V_{IN} = 0} = \frac{Z_L}{1 - G_I\, G_M\, Z_L \left(H_I + \dfrac{H_O}{G_I} \right)}$$

Figure 15 Flow Diagrams of a Multiloop Amplifier

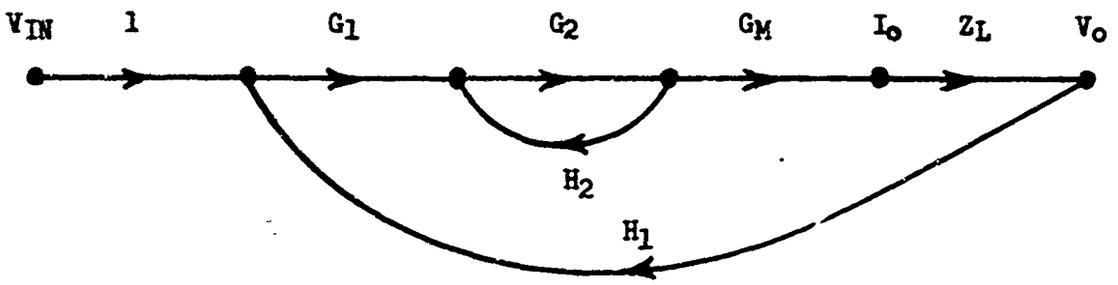

$$\frac{C}{R} = \frac{V_o}{V_{IN}} = \frac{G_1 \; G_X \; G_M \; Z_L}{1 - G_1 \; G_X \; G_M \; Z_L \; H_1}$$

Where $$G_X = \frac{G_2}{1 - G_2 \; H_2}$$

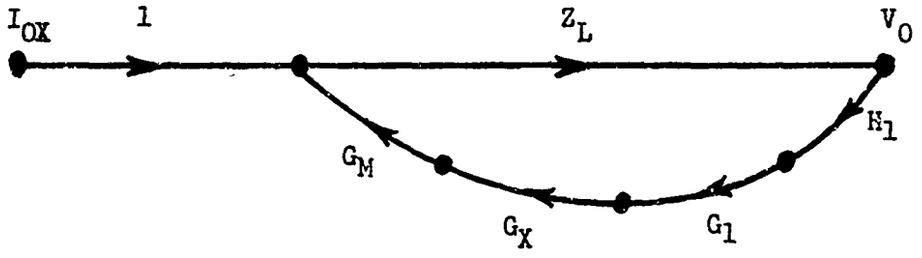

$$Z_M = \frac{Z_L}{1 - G_1 \; G_X \; G_M \; Z_L \; H_1}$$

Loop Gain = $G_1 \; G_X \; G_M \; Z_L \; H_1$

Figure 16 Flow Diagrams of an Amplifier with Internal Loop

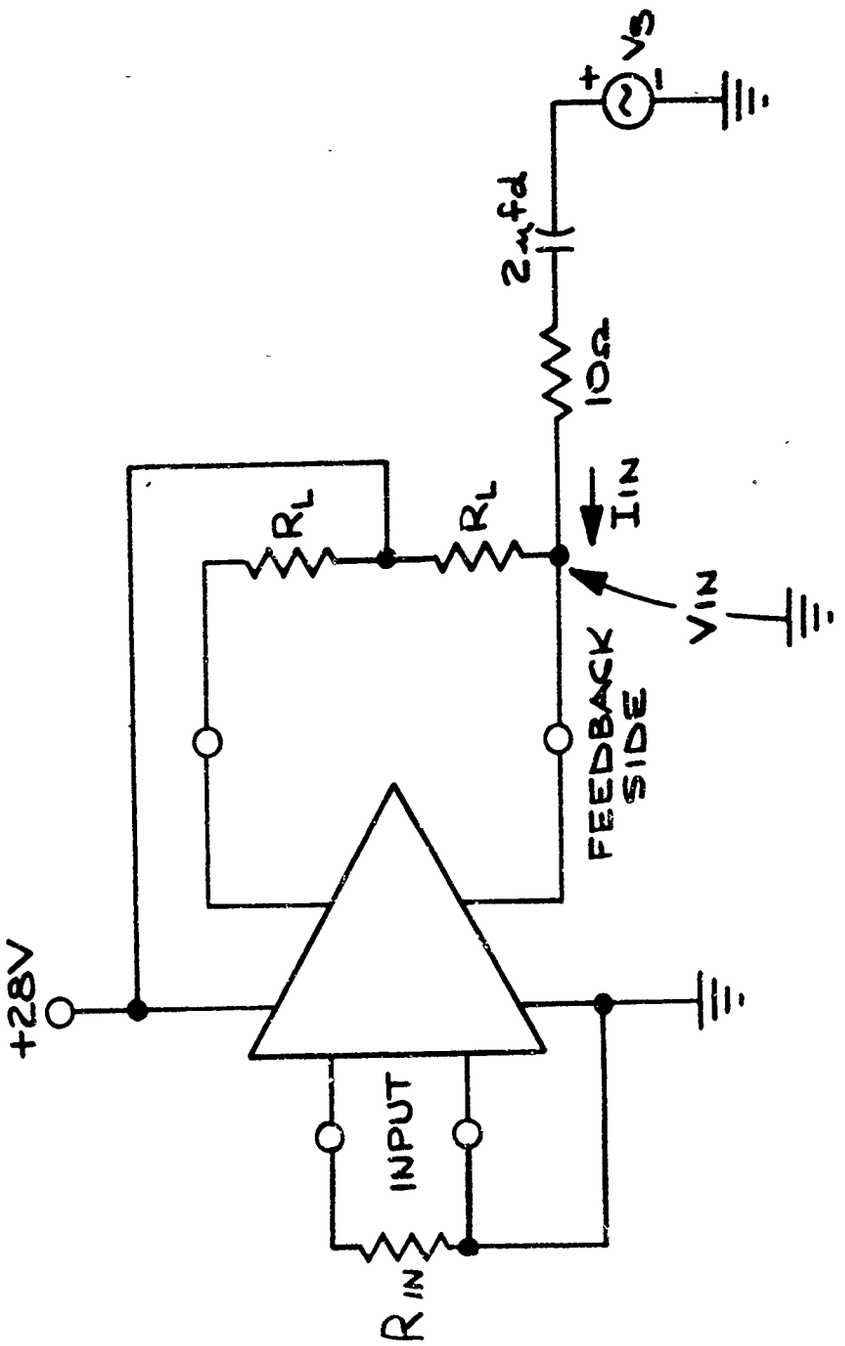

FIG 17 OUTPUT IMPEDANCE MEASUREMENT CIRCUIT

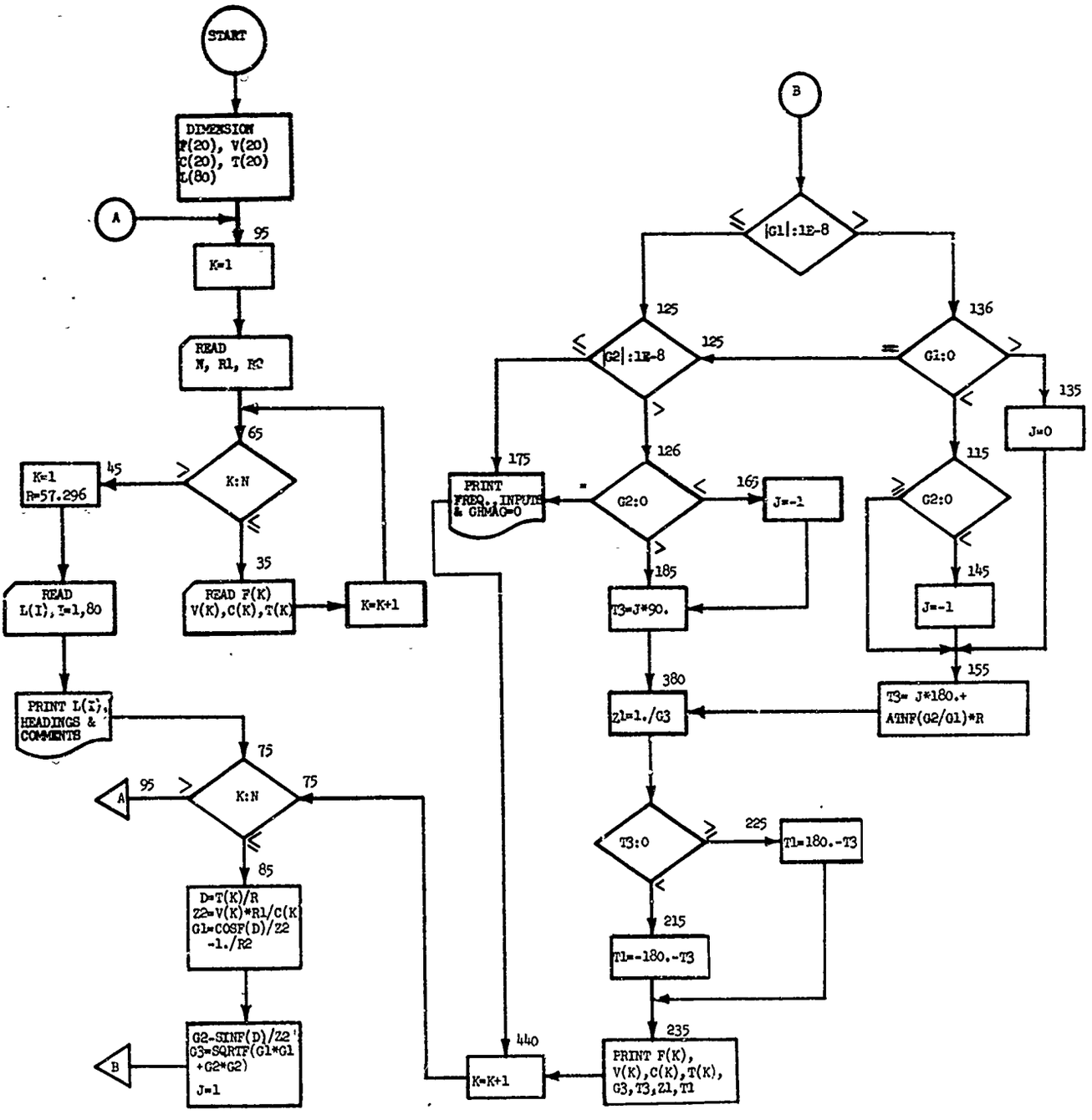

Figure 18 Flow Chart for Computation of GH and $Z_{unstable}$

```
C       F03-68-41       GH-EQU                                          000
C       PROGRAM TO CALCULATE GH MAGNITUDE AND ANGLE AND BORDERLINE      100
C       STABILITY LOAD.ON FIRST DATA CARD PUT NO OF FREQS(20 MAX),VALUE OF110
C       CURRENT SENSE RESISTOR, AND LOAD RESISTOR VALUE-(FORMAT I3,2F5.0).120
C       ON REMAINING CARDS PUT DATA IN THIS ORDER- FREQ,INPUT VOLTAGE,  130
C       CURRENT SENSE VOLTAGE, ANGLE OF INPUT WRT CURRENT SENSE VOLTAGE 140
C       -(FORMAT F8.0,3F5.0).                                           150
        DIMENSION F(20),V(20),C(20),T(20),L(80)                         160
   95   K=1                                                             170
        READ 25,N,R1,R2                                                 220
   25   FORMAT (I3,2F5.0)                                               230
   65   IF (K-N) 95,35,45                                               240
   35   READ 55,F(K),V(K),C(K),T(K)                                     250
   55   FORMAT (F8.0,3F5.0)                                             260
        K=K+1                                                           270
        GO TO 65                                                        280
   45   K=1                                                             290
        R=57.296                                                        300
        READ 46,(L(I),I=1,80)                                           302
   46   FORMAT (80A1)                                                   304
        PRINT 15,(L(I),I=1,80)                                          305
   15   FORMAT (19H1SA GH CALCULATIONS,/80A1/                           306
       1 10H FREQUENCY,7X,3HVIN,10X,3HVCS,                              307
       2 6X,11HANG VIN/VCS,4X,6HGH MAG,7X,6HGH ANG,5X,11HZ UNSTB MAG,2X,308
       3 11HZ UNSTB ANG/)                                               309
   75   IF (K-N) 85,85,95                                               310
   85   D=T(K)/R                                                        320
        Z2=V(K)*R1/C(K)                                                 330
        G1=COSF(D)/Z2-1./R2                                             340
        G2=-SINF(D)/Z2                                                  350
        G3=SQRTF(G1*G1+G2*G2)                                           360
        J=1                                                             370
        IF (ABSF(G1)-1E-8) 125,125,136                                  375
  136   IF (G1) 115,125,135                                             380
  115   IF (G2) 145,155,155                                             390
  145   J=-1                                                            400
  155   T3=J*180.+ATANF(G2/G1)*R                                        410
        GO TO 380                                                       420
  135   J=0                                                             430
        GO TO 155                                                       440
  125   IF (ABSF(G2)-1E-8) 175,175,126                                  445
  126   IF (G2) 165,175,185                                             450
  165   J=-1                                                            460
  185   T3=J*90.                                                        470
        GO TO 380                                                       480
  175   PRINT 176,F(K),V(K),C(K),T(K)                                   490
  176   FORMAT (4(PE10.4,3X),24HGH MAGNITUDE EQUALS ZERO)               500
        GO TO 440                                                       510
  380   Z1=1./G3                                                        520
        IF (T3) 215,225,225                                             530
  215   T1=-180.-T3                                                     540
        GO TO 235                                                       550
  225   T1=180.-T3                                                      560
  235   PRINT 245,F(K),V(K),C(K),T(K),G3,T3,Z1,T1                       570
  245   FORMAT (8(PE10.4,3X))                                           580
  440   K=K+1                                                           590
        GO TO 75                                                        600
        END                                                             610
```

Figure 19 Card FORTRAN Computer Program for Computation of GH and $Z_{unstable}$

```
10 REM INSERT DATA IN LINES 500 TO 800.  THE ORDER OF DATA IS-
20 REM FREQUENCY, INPUT VOLTAGE,CURRENT SENSING VOLTAGE, AND ANGLE
30 REM OF INPUT VOLTAGE WRT CURRENT SENSING VOLTAGE.
100 PRINT "PROGRAM TO CALCULATE GH MAGNITUDE AND ANGLE, AND"
105 PRINT "BORDERLINE STABILITY LOAD"
110 PRINT
120 PRINT "ENTER NO. OF FREQUENCIES, VALUE OF CURRENT SENSE RESISTOR"
121 PRINT "AND LOAD RESISTOR VALUE"
130 INPUT N,R1,R2
140 DIM F(15)
150 DIM V(15)
160 DIM I(15)
170 DIM T(15)
180 LET K=1
190 PRINT
200 PRINT "FREQ","VIN","VCS","PHASE ANGLE OF VIN WRT VCS"
210 IF K>N THEN 250
220 READ F(K), V(K), I(K), T(K)
225 PRINT F(K),V(K),I(K),T(K)
230 LET K=K+1
240 GO TO 210
250 LET K=1
260 PRINT
270 PRINT"FREQ","GH MAG","GH ANG","Z UNSTBL MAG","Z UNSTBL ANG"
280 IF K>N THEN 455
285 LET D=T(K)/57.296
290 LET Z2=(V(K)*R1)/I(K)
300 LET G1=COS(D)/Z2-1/R2
310 LET G2=-SIN(D)/Z2
320 LET G3=SQR(G1*G1+G2*G2)
330 LET J=1
335 IF G1=0 THEN 350
336 IF G1>0 THEN 345
340 IF G2<0 THEN 365
341 GO TO 370
345 LET J=0
346 GO TO 370
350 IF G2>0 THEN 360
351 IF G2=0 THEN 358
355 LET J=-1
356 GO TO 360
358 PRINT "GH MAG EQUALS ZERO"
359  GO TO 440
360 LET T3=J*90
362 GO TO 380
365 LET J=-1
370 LET T3=J*180+ATN(G2/G1)*57.296
380 LET Z1=1/G3
390 IF T3<0 THEN 420
400 LET T1=180-T3
410 GO TO 430
420 LET T1=-180-T3
430 PRINT F(K),G3,T3,Z1,T1
440 LET K=K+1
450 GO TO 280
455 PRINT
460 PRINT"IF MORE DATA NEEDS TO BE PROCESSED, TYPE IN NEW DATA AND "
461 PRINT "RUN AGAIN."
500 DATA 0
999 END
```

Figure 20 Time-Sharing BASIC Computer Program for Computation of GH and Z unstable

TABLE VI

DEFINITION OF VARIABLES USED IN COMPUTATION OF GH AND ZL (UNSTABLE)

ITEM NO.	VARIABLE	DEFINITION
1	L(I)	User information such as Mfgr., P/N, S/N, etc. (The printout will be a duplicate of the input punched on the final data card.)
2	C(K)	Current sensing voltage array
3	F(K)	Frequency array
4	T(K)	Angle of Input with respect to current sensing voltage array
5	V(K)	Input voltage array
6	D	T(K) in radians
7	G1	Real part of GH
8	G2	Imaginary part of GH
9	G3	GH magnitude
10	N	Number of frequencies
11	R	Conversion factor (radians to degrees)
12	R1	Current sensing resistor value
13	R2	Load resistor value
14	T1	Z1 unstable angle in degrees
15	T3	GH angle in degrees
16	Z1	Z unstable magnitude
17	Z2	Measured impedance at amplifier output

be identical and equal to $1/GH$. The angle of Z_{11}, which would cause borderline stability, is 180° minus the angle of GH. Also, Z_{12} has about 180° phase difference from Z_{11} at 400 hertz. It can be shown that comparing $Z_{12} \pm 180°$ with the unstable load determined from GH (non-feedback side) $\pm 180°$ will yield the correct stability information for the non-feedback side. For all of the amplifiers tested, Z_{11} never caused instabilities while Z_{12} for the one tuning capacitor case presented the greatest possibility of instability. It is for this reason that the stability predictions and calculations for this study are based only on this single tuning capacitor configuration.

D. CURVE COMPARISON

Figure 21 illustrates a composite plot versus frequency of the $-Z_{12}$ for a typical motor and the Z unstable for an amplifier. The plot of $-Z_{12}$ is presented because, as previously explained, in all the cases examined, Z_{11} never made the amplifier unstable. The loop gain which involved Z_{12} exhibited tendency for instability in both the one and two tuning capacitor cases, but the former was more severe. The stability criterion mentioned in Figure 21 indicates when the open-loop gain transfer function has no poles in the right half plane. The curve comparison technique is simply a quick method to examine the overlayed motor/amplifier characteristics to perform a simplified Nyquist stability analysis. The value of the loop gain (LG) is

$$|LG| = |Z_{12}| / |Z_{unstable}|$$

because $$|LG| = |GHZ_L|$$

and $$|Z_{unstable}| = \frac{1.0}{|GH|}$$

The $|LG| = 1$ when the magnitude curves cross, and the $\angle LG = \pm 180°$ when the phase angle curves cross. The stability criterion is determined from Nyquist stability analysis which indicates right half plane poles if the point (-1, 0) is encircled by the polar plot of LG. Further discussion of the stability criteria is presented in Chapter VII.

NOT REPRODUCIBLE

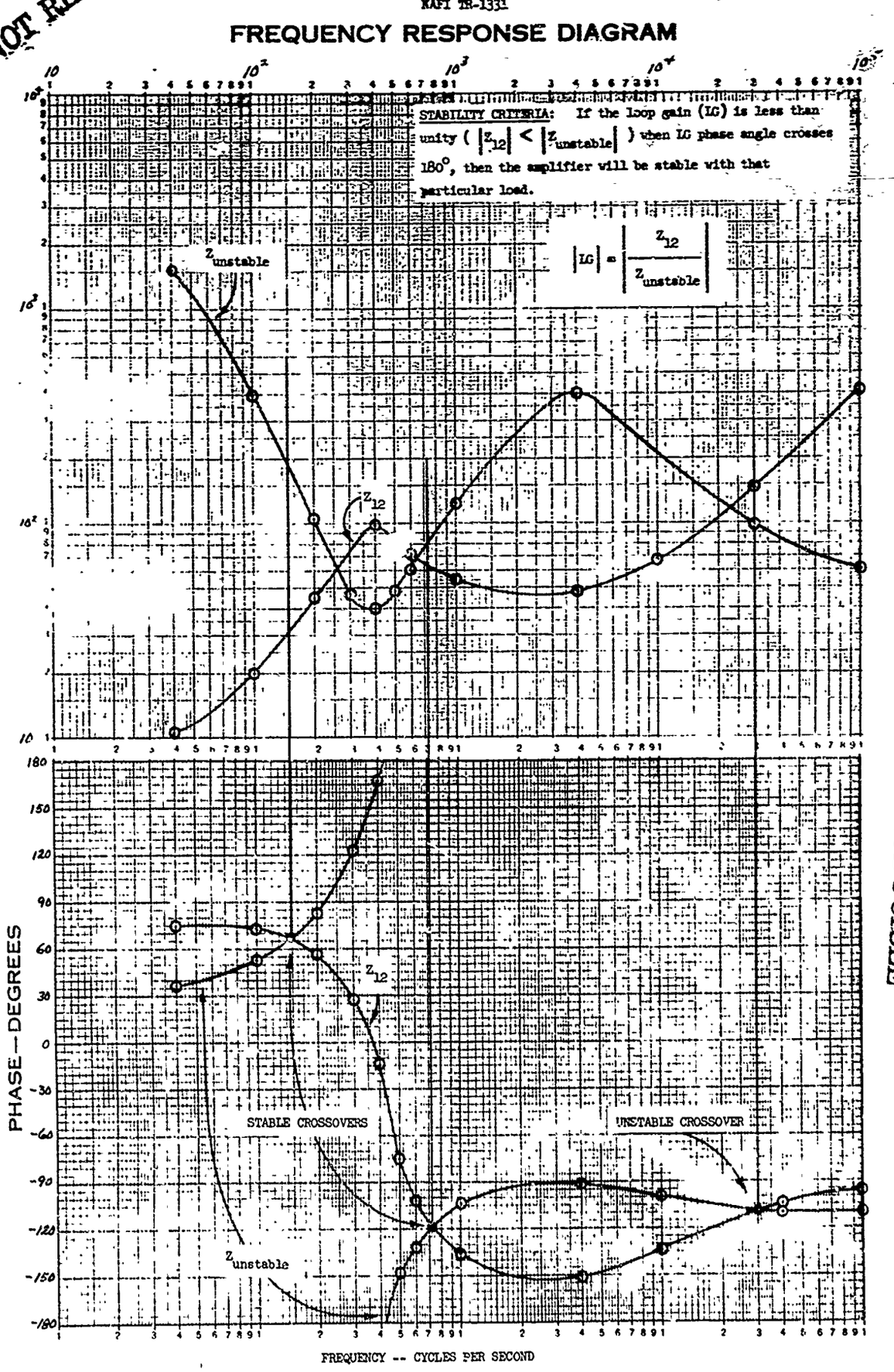

Figure 21 Comparison of Z_{12} and $Z_{unstable}$ Curves to Determine Stability

NOT REPRODUCIBLE

VII. STABILITY DETERMINATION TECHNIQUES

A. DUMMY LOAD DETERMINATION

1. Worst-Case Circuits

As explained previously, the motor equivalent series circuit parameter value limits were represented in a matrix of 16 circuit cases for each motor size (see Figure 8). The circuits in each group were converted into more complex circuits which required missing parameter value determination. The individual circuit in each group that exhibits the most unstable characteristics will represent that size motor as the worst-case stability circuit. In agreement with this, the circuit that presents the greatest opposition to amplifier output power (i.e., causes minimum output power) will be the worst-case power circuit. This worst-case condition was chosen to determine if the amplifiers could deliver an acceptable (minimum) amount of power to the load. Another possible worst-case condition is that load which causes maximum power to be delivered by the amplifier which would indicate whether the output stages could withstand maximum load current. The latter worst-case power condition was not considered in this study. This means that each of these worst-case circuits contain the worst possible parameters combination in their respective sample motor group. Since the other circuits possess better power or stability characteristics, an amplifier that operates satisfactorily with the worst-case circuits will perform better with any other sample motor within that group.

2. Dummy Loads

a. General - With dummy loads that simulate the equivalent circuit in Figure 5 for nominal, worst-case stability, and worst-case power, amplifier parameters such as stability, power output, gain, phase shift, linearity, and temperature range performance can be measured or determined. For proper dummy load simulation at temperatures above or below room temperature, the temperature-sensitive motor parameters in the equivalent circuit must be projected from their normal temperature value to the

motor test temperature. Table VII lists the worst-case dummy load parameters projected to +125°C. This permits amplifier testing at desired temperatures while the loads remain at room temperature. Also, this eliminates the improper load simulation possible with dummy load component value changes due to temperature cycling. Substituting a qualified transformer and low tolerance decade boxes for the parameters in Figure 5 would provide rapid practical motor simulation for several motor sizes with the same dummy load. With this type dummy load based on practical correlated motor specifications, incoming inspection acceptance tests can virtually assure servo amplifier/motor combination compatibility. Another very important point is that the dummy load motor parameter values have to be determined only once.

b. Computer-Aided Solution Technique - Driving-point impedance (Z_{11}) and transfer impedance (Z_{12}) are the major motor parameters as seen by the amplifier. In fact, these impedance magnitudes and angles must simulate actual motor performance for the amplifier. Worst-case motor load simulation is accomplished by reducing all of the worst-case equivalent circuit parameter values into their usable impedance equivalents (Z_{11} and Z_{12}). The magnitudes and angles are calculated by a computer program. The printout of the card fortran version and the time-sharing basic version of this program are illustrated in Figures 22 and 23. Table VIII defines the variables used in these computer programs. This program solves equations 7-1 and 7-2 for Z_{11} and Z_{12}. These equations are developed in NAFI TR-1053.

$$Z_{11} = \frac{1}{4}\left[\frac{1}{SC_T + \dfrac{1}{R_{DC} + SL - \dfrac{S^2K^2L^2}{R_R + SL}}} + R_{DC} + SL_{LP}\right] \quad (7\text{-}1)$$

$$Z_{12} = -\frac{1}{4}\left[\frac{1}{SC_T + \dfrac{1}{R_{DC} + SL - \dfrac{S^2K^2L^2}{R_R + SL}}} - R_{DC} - SL_{LP}\right] \quad (7\text{-}2)$$

TABLE VII Worst-Case Dummy Loads

(PARAMETER VALUES ARE PROJECTED TO +125°C AMBIENT)

SERIES EQUIVALENT					COMPLEX EQUIVALENT					
TYPE LOAD	CASE NO.	R_{DC} (OHMS)	R_{AC} (OHMS)	X_{LS} (OHMS)	R1(R_{DC}) (OHMS)	L1 (mh)	K	L (mh)	R_R (OHMS)	C_T (uf)
WORST	871	168	44.1	220.7	168	2.6	.6	129	148.5	1.43
CASE	1171	69.5	139.4	253.3	69.5	2.6	.8	171.8	309.5	1.65
STABILITY	1571	27.5	57.3	123.5	27.5	2.6	.76	82.5	153.1	3.3
WORST	870	168	44.1	220.7	168	2.6	.6	129	148.5	1.17
CASE	1170	69.5	139.4	253.3	69.5	2.6	.8	171.8	309.5	1.35
POWER	1540	10	55.8	179.8	10	2.6	.7	104.9	156.5	2.7

```
C     F-07-68-22                                                        00
      DIMENSION F(13)                                                   10
C     PROGRAM CONVERTED FROM TIME-SHARING PROGRAM Z12EQU                20
      READ 40,(F(I),I=1,13)                                             30
   40 FORMAT (13F6)                                                     90
   45 READ 50,N,R1,EL1,EL,R4,CAY,C                                      100
   50 FORMAT (I6,F6.2,F6.3,F6.4,F6.1,F6.2,E9.2)                         110
      IF((N/10)*10-N)60,80                                              120
   60 PRINT 70,N                                                        130
   70 FORMAT (////24X,9HCASE NO. ,I4//)                                 140
      GO TO 95                                                          150
   80 PRINT 82                                                          160
   82 FORMAT (1H1,2X,60HSERVO MOTOR DRIVING-POINT (Z11) AND TRANSFER IMP162
     1EDANCE (Z12))                                                     163
      PRINT 90,N                                                        165
   90 FORMAT (//24X,9HCASE NO. ,I4,//)                                  170
   95 PRINT 100                                                         180
  100 FORMAT(4X,9HFREQUENCY,4X,8HZ11(MAG),4X,8HZ11(ANG),4X,8HZ12(MAG),4X190
     28HZ12(ANG),4X,8HPWR LOAD/)                                        200
      I = 1                                                             210
  110 W = 2*3.14159265*F(I)                                             220
      EL4 = (1-CAY)*EL                                                  230
      EL6 = EL4-EL1                                                     240
      EL5 = CAY*EL                                                      250
      EM4 = R4*R4+(W*EL4)**2                                            260
      E5 = R4/EM4                                                       270
      EYE5 = 1/(W*EL5)+W*EL4/EM4                                        280
      EM5 = E5*E5+EYE5*EYE5                                             290
      E3 = E5/EM5                                                       300
      EYE3 = EYE5/EM5+W*EL6                                             310
      E7 = R1+E3                                                        320
      EYE7 = W*EL1+EYE3                                                 330
      EM7 = E7*E7+EYE7*EYE7                                             340
      E8 = E7/EM7                                                       350
      EYE8 =-(EYE7/EM7-W*C)                                             360
      EM8 = E8*E8+EYE8*EYE8                                             370
      E9 = (R1-(E8/EM8))/4                                              380
      EYE9 = (EYE8/EM8+W*EL1)/4                                         390
      Z9 = SQRTF(E9*E9+EYE9*EYE9)                                       400
      T9 = ATANF(EYE9/E9)*57.296                                        410
      J = 0                                                             420
      J1 = 1                                                            430
      IF(E9)279,278                                                     450
  278 J = 1                                                             460
  279 IF(EYE9)281,280                                                   470
  280 J1 = -1                                                           480
  281 T9 = T9+J*J1*180                                                  490
      P1 = (R1+E8/EM8)/4                                                500
      P2 = (W*EL1-EYE8/EM8)/4                                           510
      P3 = SQRTF(P1*P1+P2*P2)                                           520
      P4 = ATANF(P2/P1)*57.296                                          530
      P5 = P3*COSF(P4/57.296)                                           532
      PRINT 340,F(I),P3,P4,Z9,T9,P5                                     540
  340 FORMAT (I11,F14.4,4F12.4)                                         550
      IF (I-13)350,45                                                   560
  350 I = I+1                                                           570
      GO TO 110                                                         580
      END                                                               590
```

Figure 22 Printout of Program to Calculate Load Impedances Z_1 and Z_2 (Card FORTRAN Version)

```
10  REM PROGRAM TO CALCULATE CM DRIVING-POINT(Z11) AND TRANS-
020 REM FER (Z12) IMPEDANCES. ENTER DATA IN LINES 900-998 IN
030 REM THE FOLLOWING ORDER: INIT. FREQ.,RDC,LEAKAGE,L,RZTAP
040 REM RES.,K,CAP.,NO. OF ADDITIONAL FREQS,ADDITIONAL FREQ
050 REM VALUES. ENTER CASE # IN LINE 800
060 LET I=1
100 READ X,F,R1,L1,L,R4,K,C,N
102 PRINT
104 PRINT "CASE";X
106 PRINT
110 PRINT "FREQUENCY","Z11(MAG)","Z11(ANG)","Z12(MAG)","Z12(ANG)"
112 PRINT
120 LET W=2*3.14159265*F
130 LET L4=(1-K)*L
140 LET L6=L4-L1
150 LET L5=K*L
160 LET M4=R4*R4+(W*L4)^2
170 LET E5=R4/M4
180 LET I5=1/(W*L5)+W*L4/M4
190 LET M5=E5*E5+I5*I5
200 LET E3=E5/M5
210 LET I3=I5/M5+W*L6
220 LET E7=R1+E3
230 LET I7=W*L1+I3
240 LET M7=E7*E7+I7*I7
250 LET E8=E7/M7
260 LET I8=(I7/M7-W*C)*(-1)
270 LET M8=E8*E8+I8*I8
271 LET E9=(R1-E8/M8)/4
272 LET I9=(I8/M8+W*L1)/4
273 LET Z9=SQR(E9*E9+I9*I9)
274 LET T9=ATN(I9/E9)*57.296
275 LET J=0
276 LET J1=1
277 IF E9<0 THEN 279
278 LET J=1
279 IF I9<0 THEN 281
280 LET J1=-1
281 LET T9=T9+J*J1*180
283 LET P1=(R1+E8/M8)/4
285 LET P2=(W*L1-I8/M8)/4
288 LET P3=SQR(P1*P1+P2*P2)
290 LET P4=ATN(P2/P1)*57.296
330 PRINT F,P3,P4,Z9,T9
340 IF I>N THEN 999
350 READ F
360 LET I=I+1
370 GO TO 120
800 DATA 170
900 DATA 1200
902 DATA 64
904 DATA 3E-3
906 DATA .107,217,.73
912 DATA 1.53E-6
914 DATA 2,400,100
999 END
```

Figure 23 Printout of Program to Calculate Load Impedances Z_{11} and Z_{12} (Time-Sharing BASIC Version)

TABLE VIII

DEFINITION OF VARIABLES USED IN THE COMPUTATION OF Z_{11} AND Z_{12}

ITEM NO.	INPUT VARIABLE		DEFINITION
	CARD FORTRAN	TIME SHARING BASIC	
1	CAY	K	The coupling coefficient between the stator & rotor.
2	C	C	Tuning capacitor value.
3	EL1	L1	Leakage inductance.
4	EL	L	Magnetizing inductance.
5	N	X	Case no.
6	R1	R1	R_{DC}
7	R4	R4	R_R = Rotor resistance.

c. Worst-Case Stability - The impedance (magnitude and angle) of $-Z_{12}$ for each different combination of extreme motor parameters (see Figure 8) were compared with the amplifier $Z_{unstable}$ (magnitude and angle) at various frequencies. The combination of motor parameters which resulted in the greatest possiblity of causing instability was the set of parameters which resulted in the largest absolute value of the angle of (Z_{12}) near 1200 hertz. This most unstable condition occurred with the amplifier at maximum temperature and the motor equivalent circuit projected from the average motor ambient temperature to this maximum temperature. The following conditions were the same for sizes 8, 11, and 15 servomotors:

(1) The matrix case number was 71. Checking this case number in the matrix of possible loads (Figure 8) shows that the equivalent circuit parameter values for the worst-case stability dummy load have definite value trends: R_{DC}, X_{LS}, and C_T are maximum, and R_S is minimum.

(2) The operating temperature was maximum. Generally, as the amplifier $Z_{unstable}$ magnitude and absolute value of angle $Z_{unstable}$ decrease with increasing temperature, the motor Z_{12} magnitude and absolute value of the angle of Z_{12} increases with increasing temperature. Thus, the possibility that instability may occur increases. This shows that an amplifier/motor combination operating normally at room temperature can very easily become unstable at increased temperatures.

d. Worst-Case Power - As previously mentioned, the worst-case power equivalent motor circuit as defined in this report causes minimum amplifier output power. The matrix case numbers that fulfilled this requirement contained the maximum real component of driving-point impedance (Z_{11}) (i.e., the maximum $|Z_{11}|$ Cos $\angle Z_{11}$). Like the worst-case stability tests, the worst-case (W.C.) power conditions occur at maximum temperature. These worst-case circuit values are also projected to their proper values at the maximum motor operating temperature. The sizes 8 and 11 worst-case power circuits are the same as the sizes 8 and 11 worst-case stability circuits, respectively, with one exception. The tuning capacitor (C_T)

value is minimum for W.C. power and maximum for W.C. stability. For the size 15 motors, the W.C. power dummy load corresponded to case 40 of the matrix in Figure 8. The equivalent circuit parameters corresponding to this case are: R_s is a maximum; R_{DC}, X_{LS}, and C_T are a minimum. Table IX below reviews the worst-case power dummy load parameter conditions.

TABLE IX PARAMETER LIMITS FOR WORST-CASE POWER DUMMY LOADS

Item	Parameter	Size 8 & 11 Motors	Size 15 Motor
1	Matrix Case No.	70	40
2	Temperature	Max	Max
3	R_{DC}	Max	Min
4	R_S	Min	Max
5	X_{LS}	Max	Min
6	C_T	Min	Min

3. Load Implementation

Once these worst-case and nominal load parameters are determined, there still remains the problem of implementing the load by actual components for laboratory tests. The most difficult item in the equivalent circuit to simulate is the ideal transformer. The CODED-"T" automatic transformer design computer program was used to obtain a design which would approximate the ideal transformer characteristics. Figure 24 is the computer printout of the performance and construction data for the transformer design which was used for the simulation of all three sizes of motor loads. The resistances in the dummy loads were simulated by selected carbon composition resistors and the inductances by decade inductance boxes. The transformer leakage inductance was used to represent the leakage between halves of the control winding. When calculating the values for the external resistors and inductors,

```
                                POWER TRANSFORMER DESIGN READOUT

PART 1 - CONSTRUCTION PARAMETERS
A, IDENTIFICATION
    CODED SERIAL NUMBER = 71846
B, MATERIAL
    1, TEMPERATURE CLASS = F
    2, CORE= 4 MIL TAPEWOUND C-TYPE CORE CATALOGUE NO, M188  SINGLE PHASE        BUWEPS 61A5A132- 25 LAST NO, 25
    3, COIL FORM   1,562 BY 0,781 BY 3,000 BY 0,032 (INCHES)                     BUWEPS 60A5A274- 18
    4, WIRE                                          POLYTHERMALEZE              BUWEPS 61A5A9
    5, INSULATION                                SILICONE VARNISHED GLASS        BUWEPS 61A5A169
    6, IMPREGNANT                                             EPOXY              BUWEPS 64A5A9-1
    7, ENCAPSULANT                                  THIXOTROPIC EPOXY           BUWEPS 60A5A80-1
    8, SOLDER - SPLICES AND BAND SEAL                 5 PCT, TIN ALLOY          QQ-S-571 TYPE SN5WS
    9, ADHESIVE TAPE                             SILICONE VARNISHED GLASS        BUWEPS 61A5A157- 3
                                                                                 MIL-F-14256 TYPE A
   10, FLUX
   11, BRACKETS                                                                  BUWEPS 57A5A256
   12, BAND NO,                                                                  BUWEPS 57A5A258
   13, SEAL NO,
C, CONSTRUCTION
    1, COIL (START ALL WINDINGS AT SAME END OF COIL UNLESS OTHERWISE SPECIFIED,)
       WINDING TYPE= SINGLE PHASE   SINGLE COIL
       NO, OF COILS REQUIRED 1
       WINDING NUMBER,,,,,,,,,,,,,,        1        2        3        4        5        6        7        8        9
    2, WIRE
       GAGE (DRAWING DASH NO,),,,,       22       24
       TURNS PER WNDG PER COIL,,,       598      628
       TAP AT TURNS,,,,,,,,,,,,,,,      299        0
       TURNS PER LAYER,,,,,,,,,,,,       86      105
       LAYERS REQUIRED,,,,,,,,,,,,        7        6
       MARGIN (INCHES),,,,,,,,,,,,,  0,197    0,220
       MAX, WIRE LENGTH (FEET),,,,      279      390
    3, INSULATION
       INTERLAYER INSUL, (MILS),,,        5        5
       LAYERS REQUIRED,,,,,,,,,,,,
       INTERWNDG, INSUL, (MILS),,,        5        0
       LAYERS REQUIRED,,,,,,,,,,,,
       INSULATION (COIL TO COIL FORM),,,,,,, NONE REQUIRED
       OUTER WRAP OVER COIL,,,,,,,,,,,,,,,
```

POWER TRANSFORMER DESIGN READOUT

PART 2= ELECTRICAL PARAMETERS (CODED SERIAL NUMBER= 71046)

A, WINDING RATINGS

	1	2	3	4	5	6	7	8	9
WINDING NUMBER									
WINDING DESIGNATION	PRIM	SEC; 1							
POWER (VOLT=AMPS)	72;4	67;0							
VOLTAGE RATINGS									
FULL LOAD VOLTAGE	115;0	111;7							
NO LOAD VOLTAGE	115;0	120;8							
TAP AT VOLTS	57;5	0;9							
VOLTAGE REGULATION (PCT;)		8;2							
TOLERANCE REQUESTED (PCT;)		5;0							
CURRENT RATINGS (MILLIAMPS)									
RMS CURRENT	667;0	600;0							
DC= CURRENT	10;0	0;0							
IMPEDENCE (OHMS)									
WINDING RESISTANCE	4;6	9;6							
RESISTIVE LOAD		184;1							
CAP; REACTANCE TO CORE	2885;3	3893;9							
PARAMETERS OF SECONDARIES REFERRED TO THE PRIMARY									
PHASE SHIFT (DEGREES)		=4;8							
LEAKAGE INDUCT; (MILHYS)		4;3							
INDUCTIVE REACTANCE (OHMS)		10;9							
INTERWINDING CAP; (MMF)		1987;2							
CAP; REACTANCE (KILOHMS)		153;2							

B, SIZE (MAXIMUM) DOES NOT INCLUDE ENCAPSULATION; BAND SEAL; BRACKETS; OR TERMINAL BULGE,

VOLUME	55;378	CUBIC INCHES
OVERALL DIMENSIONS		
HEIGH; (E DIRECTION)	3;506	INCHES
WIDTH (D DIRECTION)	3;508	INCHES
LENGTH (G DIRECTION)	4;526	INCHES

C, GENERAL RATINGS

EFFICIENCY	92;5	PERCENT
FLUX DENSITY	16545;	GAUSS
MAXIMUM FREQUENCY	4000;0	CPS
MINIMUM FREQUENCY	40;0	CPS
RESONANT FREQUENCY	39173;	CPS
AMBIENT TEMPERATURE	100;	DEGREES
TEMPERATURE RISE	16;	DEGREES
TEMPERATURE CLASS	F	
OPERATING LIFE	200000;	HOURS

D, GENERAL PARAMETERS

CORE LOSS	0;0	WATTS	CORE LOSS CURRENT (NOM;)	0;003	AMPS
COPPER LOSS	5;4	WATTS	MAGNETIZING CURRENT (MAX;)	0;216	AMPS
EXCITATION LOSS	3;9	VOLT=AMPS	IRON SHUNT RESISTANCE	OVER 99999	OHMS
MAGNETIZING VARS	2;7	VOLT=AMPS	IRON SHUNT REACTANCE	4863;	OHMS

MART TR-1331

57

Figure 24 Continued

the effect of the transformer internal parameters (e.g., secondary leakage, R_{bc}, and turns ratio) should be compensated for when possible, for more accurate simulation.

The magnetizing impedance of the transformer is high compared to the secondary load, so the leakage inductances, DC resistances, and turns ratio are the only parameters of significance. The experimentally determined transformer parameters are:

DC resistance (pri.)	=	4.5 ohms
DC resistance (sec.)	=	9.3 ohms
Leakage inductance (pri.)	=	2.6 mh
Leakage inductance (sec.)	=	2.6 mh
Turns ratio (N_p/N_s)	=	0.907:1

4. Load Comparisons (Practical, Ideal, and Experimental)

Once the parameter values were calculated for the loads using practical components, an analysis of Z_{12} versus frequency using the CODED computer circuit analysis program for the practical loads (Figure 26) was performed and compared with the desired frequency responses of the ideal loads (see Figure 5). These loads were constructed in the laboratory, and the Z_{12} responses were determined experimentally. Figure 25a illustrates the comparisons between the Z_{12} responses for the ideal (Figure 5), practical (Figure 26), and experimental (Figure 27) worst-case stability loads for size 8 motors. It is thought that the reason for the disagreement in the experimental curve at high frequencies is caused by inaccurate prediction of the transformer distributed capacitances which have a significant effect.

Also, on the same drawing the Z_{12} of the practical equivalent series dummy load (Figure 28a) is plotted to illustrate the differences. It should be noted that the equivalent series dummy load differs significantly from the others at frequencies below the carrier frequency. The importance of this will be discussed later. Figure 25b also illustrates

these differences and the effect of changes in K for complex loads. The Z_{12} curves in Figure 25b are for ideal dummy loads for the size 8 motor.

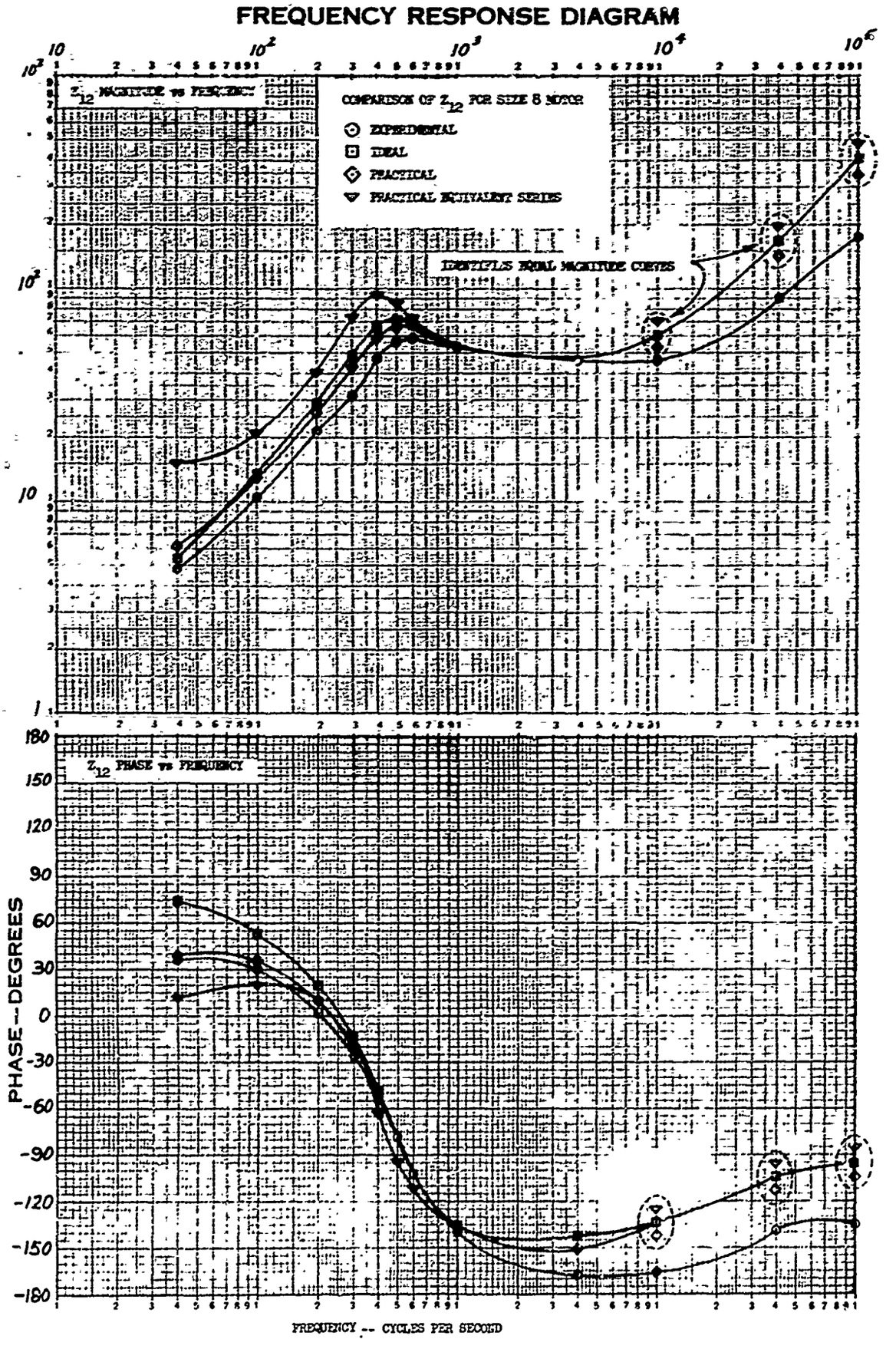

Figure 25a Comparison of Z_{12} Responses

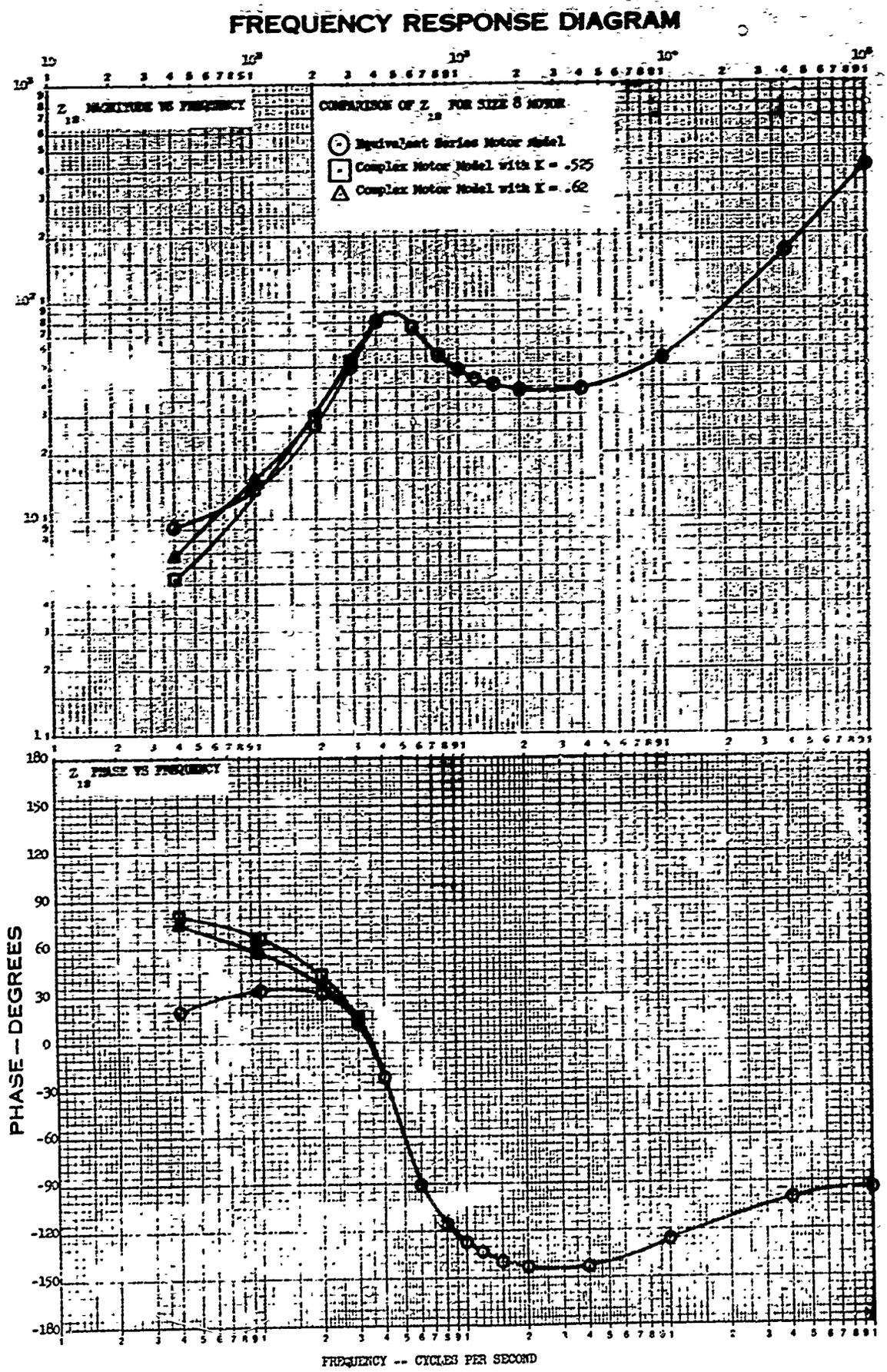

Figure 25b Comparison of Z_{12} Responses

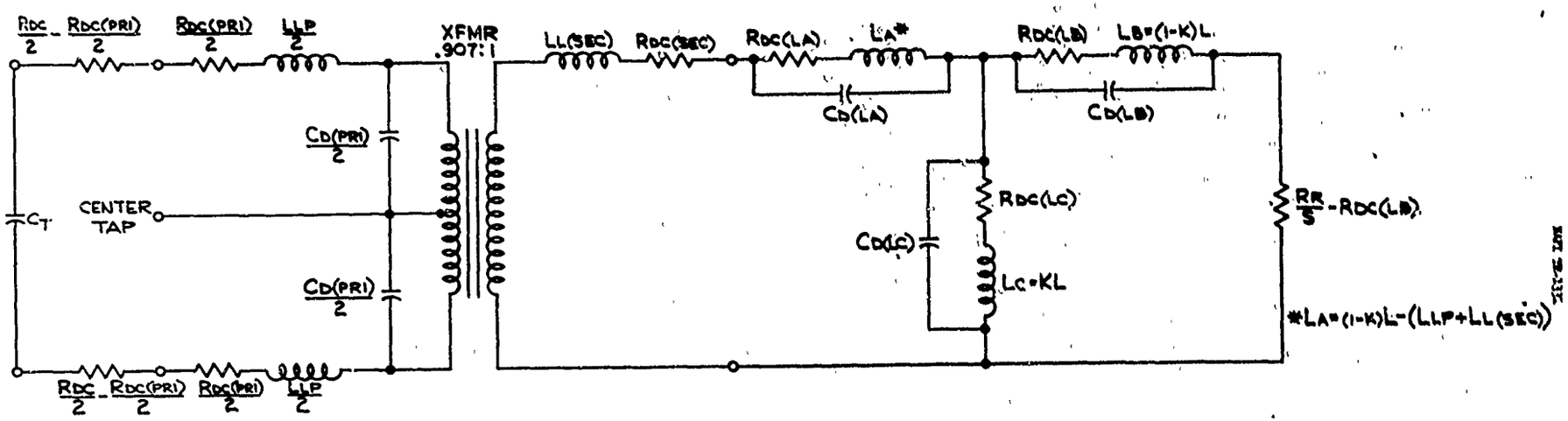

FIG. 26 PRACTICAL DUMMY LOAD FOR THE COMPLEX EQUIVALENT CIRCUIT MOTOR MODEL

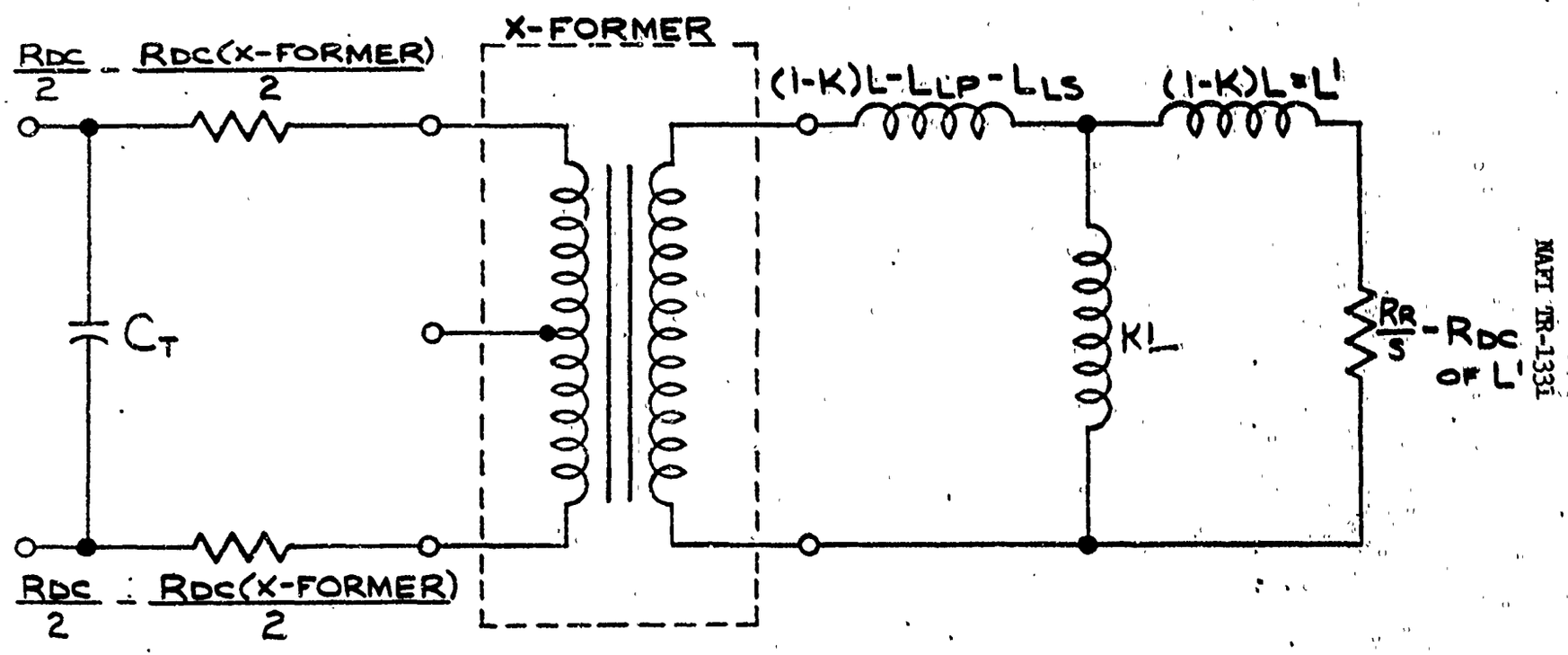

MAPI TR-1331

FIG. 27 EXPERIMENTAL DUMMY LOAD FOR THE EQUIVALENT CIRCUIT MOTOR MODEL

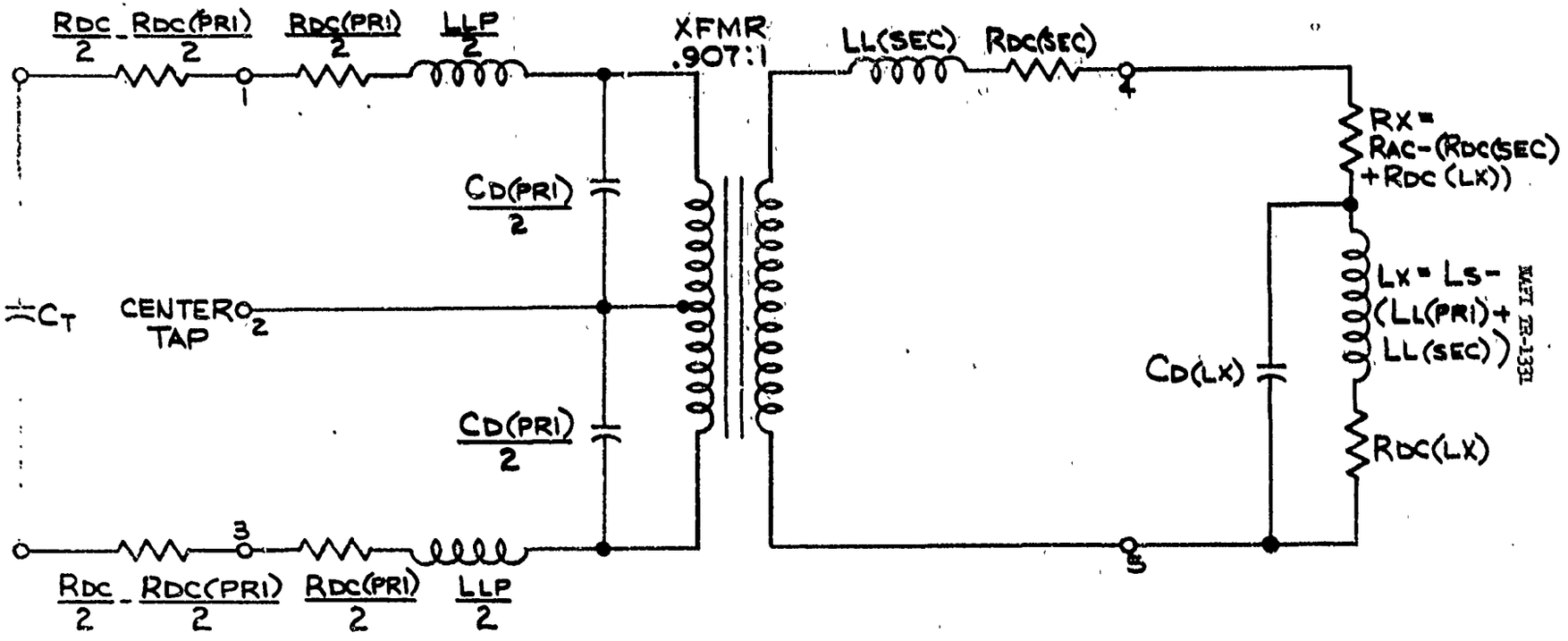

MIT ER-1331

FIG. 28a. PRACTICAL EQUIVALENT SERIES DUMMY LOAD

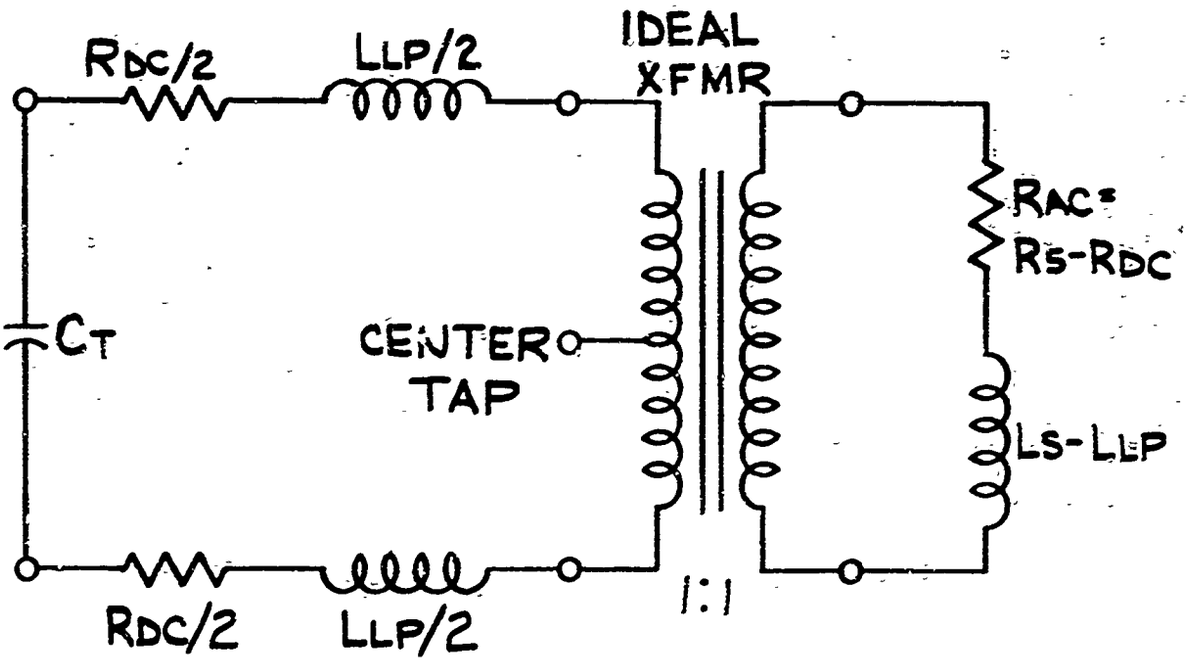

FIG. 28b. IDEAL EQUIVALENT SERIES DUMMY LOAD

B. TESTING PROCEDURE (AMPLIFIER WITH WORST-CASE DUMMY LOAD)

All of the amplifiers which have an output power rating of approximately 3.5 watts were tested with the size 8 and size 11 servo-motor dummy loads while all of the high-powered amplifiers were tested with only the size 15 dummy load. Since the worst-case (as far as stability is concerned) is when the amplifier temperature is highest (resulting in highest amplifier gain), the amplifiers were all placed in an oven at their maximum rated case temperatures. To avoid having to implement a dummy load which duplicated the motor temperature dependence characteristics, the dummy load was kept outside the oven. All temperature dependent parameter values of the equivalent circuit were projected up in temperature to the maximum. This maximum motor temperature was determined by adding the temperature rise caused by the fixed phase winding being energized to the maximum ambient temperature (+125°C) for the motors.

With the amplifier and dummy load at the proper temperatures, a transfer characteristic plot (see Figures 30, 31, and 32) was made utilizing a demodulator test set designed and built at NAFI and a X-Y recorder. A great deal of information can be obtained from these plots such as low frequency stability, gain, gain linearity, phase shift, saturated output voltage, and cross-over distortion. The function of the demodulator test set is to provide an amplitude modulated input 400 Hz signal to the amplifier and to demodulate both the input signal and the amplifier output signal. The test set provides DC output signals for the X-Y recorder which are proportional to both the in-phase and quadrature components of the demodulated signals.

C. COMPARISON OF PLOTS OF Z (unstable) AND Z_{12} FOR WORST-CASE STABILITY DUMMY LOAD

To understand how stability information may be derived from a comparison of the Z (unstable) curve and the Z_{12} curve for the worst-case

stability dummy load, the definition of Z (unstable) must be recalled. The total amplifier feedback loop gain is defined as $G(S)H(S)Z_L(S)$ where $Z_L(S)$ is the complex load on the amplifier, and $G(S)H(S)$ is independent of the load. For a given frequency, a value of the GH product may be determined experimentally, and a value of Z_L can be calculated from the characteristic equation: $GHZ_L + 1 = 0$. This value of Z_L is that which causes borderline instability and is called Z' (unstable).

Information similar to that obtained from Nyquist stability plots can be obtained from the comparison of these curves. The following equations indicate that the loop gain magnitude at any given frequency is $|Z_L| / |Z \text{ (unstable)}|$.

$$|Z \text{ (unstable)}| = \frac{|-1.0|}{|G||H|} \tag{7-3}$$

$$|\text{loop gain}| = GHZ_L \tag{7-4}$$

$$\therefore |\text{loop gain}| = \frac{|Z_L|}{|Z \text{ (unstable)}|} \tag{7-5}$$

Also, the phase angle of the loop gain can be shown to be plus or minus 180° when the Z_{12} curve crosses Z (unstable). Therefore, a polar plot of the loop gain can be considered to encircle the point (-1, 0), which indicates instability on a Nyquist plot, when the loop gain magnitude is greater than one ($|Z_{12}| > |Z \text{ (unstable)}|$) at a frequency when the loop gain phase angle is plus or minus 180° (at a crossover of the phase curves). Figure 21 illustrates two stable crossovers and one unstable crossover. One cannot blindly assume that meeting the above criteria for encircling the point (-1, 0) will ensure instability. The actual Nyquist plot (a polar plot of the loop gain) should be sketched from the Z_{12}, Z (unstable), and GH curves or values. As indicated above, the loop gain magnitude and the points where the loop gain angle equals ± 180° can be easily extracted from the comparison of Z_{12} and Z (unstable) curves. The loop gain phase angle for any given frequency would be the sum of the phase angles of GH and Z_{12}. This sketch of the Nyquist plot should be made at least once for each new amplifier configuration to ensure whether the curve will encircle the point (-1, 0) in the proper direction or not. For example, the polar plots in Figure 29 (a) and (b) of loop gain pro-

gressing in the direction of increasing frequency, are, respectively, encircling and not encircling the point (-1,0).

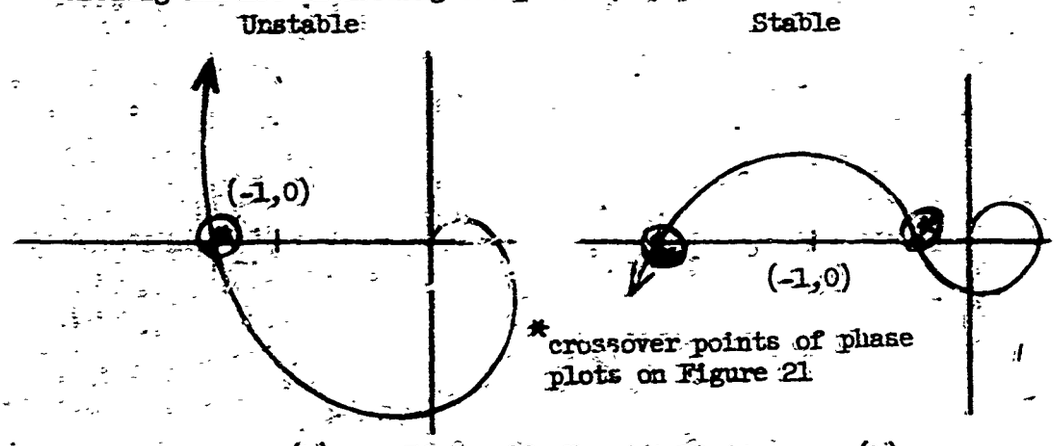

(a) Figure 29 Nyquist Plots (b)

It was noted when comparing these curves that instabilities never occurred for frequencies below 400 hertz. It should also be noted from the curves in Figure 25 that the equivalent series dummy load (Figure 28) Z_{12} curve closely matches the more complex dummy load (Figure 26) Z_{12} curve for frequencies above 400 hertz. Had these facts been known before the testing for this study, the worst-case stability dummy load utilized could have been the simpler equivalent series model (Figure 28). However, to ensure that the dummy load is worst-case for all the frequencies of probable instability, the more complex dummy load (Figure 26) is recommended and was utilized. The simpler equivalent series dummy is, however, fully adequate for nominal and worst-case power dummy load tests on amplifiers, where the 400 hertz value of the load impedance is of primary importance. The more complicated dummy load was utilized for the worst-case power testing because the parameters for this load differed from the worst-case stability load by only the capacitor value for the sizes 8 and 11 motors. The amplifiers were not tested with nominal dummy loads.

D. COMPARISON OF THE RESULTS OF THE TWO STABILITY DETERMINATION TECHNIQUES

Table X lists the servo amplifiers that were tested. Table XI

TABLE X. Servo Amplifiers Tested

IDENTIFICATION CODE	MANUFACTURER	MODEL NO.	SERIAL NO.	TYPICAL LOAD MOTOR SIZE
A	BECKMAN INSTR. INC.	961	19	8 or 11
B	"	962	21	"
C	BULOVA ELEC. DIV.	261	664440	"
D	"	261	664457	"
E	CLIFTON PRECISION PRODUCTS CO., INC.	41100000	2860	"
F	"	41100000	4486	"
G	CONTROL TECHNOLOGY CO., INC.	200HS	1074	"
H	"	200HS	1075	"
I	"	930	162	"
J	"	930	163	"
K	KEARFOTT DIVISION	C703105009	100	"
L	"	C703105009	101	"
M	"	C703148006	105	"
N	"	C703148006	126	"
O	"	C703516001	1329	15
P	MAGNETICO, INC.	T-256	8	15
Q	"	T4-3A	2016	8 or 11
R	"	T4-3A	2312	"
S	WESTON INSTR. INC.	U210914-5-25-1-2	20096	"
T	"	U210914-5-25-1-2	20097	"
U	"	U207683-3-40-1-2	20188	15

NAFI TR-1331

summarizes the stability and power output information obtained from the transfer function characteristics for each amplifier. To evaluate the accuracy of stability predictions using worst-case dummy load testing, the stability prediction information from the frequency responses and from the transfer function plots utilizing dummy loads are summarized and compared in Table XII. Out of a possible total of 38 correlations (matching stability predictions), there were 30 (79% of the total) correlations and 5 (13% of the total) borderline situations. There were only 3 (8% of the total) disagreements in the stability predictions. The reasons for the disagreements were not determined, but only two different amplifiers are involved. The Nyquist plots of these amplifiers were made, but the stability predictions did not change.

It is felt that there is sufficient correlation between the two stability testing methods to allow confidence in the stability predictions utilizing worst-case stability dummy loads. However, if test equipment similar to the demodulator test set is used to determine stability, an oscilloscope should also be used to monitor the amplifier output voltage to detect low level oscillations at frequencies above 400 hertz. These high frequency oscillations would be filtered out by the demodulator if they did not affect the amplitude of the carrier signal significantly.

TABLE XI Transfer Function Plot Characteristics

IDENTIFICATION CODE	LOAD SIZE	WORST CASE STABILITY DUMMY LOAD			WORST CASE POWER DUMMY LOAD		POWER OUT (IN PHASE)
		STABILITY	GAIN LINEARITY		PHASE SHIFT		
			condition	max. linear ampl.	LINEAR	SATURATED	
A	8	LLO	SLNL	16.5V	+7.55°	+7.67°	2.1W
	11	LLO	L	22V	+7.85°	+25.5°	2.5W
B	8	LLO	L	24V	+10.1°	+33.65°	1.8W
	11	S	L	25.5V	+9.22°	+35.2°	2.2W
C	8	LLO	L	17V	-17.2°	-24.2°	2.0W
	11	LLO	L	25.5V	-10.3°	-30.4°	2.8W
D	8	LLO	L	16.5V	-4.21°	-22.2°	2.3W
	11	LLO	L	27.5V	-3.34°	-23.2°	3.0W
E	8	S	L	22.5V	-7.66°	-19.5°	2.4W
	11	S	L	32V	-7.4°	-18.05°	3.3W
F	8	S	CD/L	12V	+7.0°	-7.6°	1.7W
	11	S	CD/L	13.5	+3.24°	-11.32°	1.0W
G	8	S	L	21V	-14.04°	-39.9°	1.4W
	11	S	L	32V	-6.45°	-36.86°	2.2W
H	8	S	L	22V	-24.8°	-44.0°	1.3W
	11	S	L	33V	-6.3°	-46.25°	1.6W
I	8	S	SLNL	25V	-34.8°	-19.4°	2.4W
	11	LLO	L	27.5	-30.0°	-19.25°	3.3W
J	8	HLO	SENL	0	PNA-HLO	-23.0°	2.5W
	11	HLO	SENL	0	PNA-HLO	-18.9°	3.3W
K	8	HLO	SENL	3V	+13.15°	+18.6°	2.3W
	11	LLO	L	29V	+2.57°	+18.05°	3.1W
L	8	HLO	SENL	6V	+16.1°	+18.2°	2.4W
	11	LLO	L	30	+3.11°	+18.1°	3.1W
M	8	S	L	22.5V	-1.72°	+0.94°	2.7W
	11	LLO	SLNL	12V	+3.1°	+1.84°	3.6W
N	8	LLO	SLNL	8V	-1.85°	+6.78°	2.6W
	11	LLO	SLNL	6V	+4.0°	+7.83°	3.6W

TABLE XI (Continued)

IDENTIFICATION CODE	LOAD SIZE	WORST CASE STABILITY DUMMY LOAD			WORST CASE POWER DUMMY LOAD		POWER OUT (IN PHASE)
		STABILITY	GAIN LINEARITY		PHASE SHIFT		
			condition	max. linear ampl.	LINEAR	SATURATED	
O	15	CNA	-	-	CNA	-	-
P	15	HLO	SENL	5V	PNA-HLO	+24.7°	2.2W
Q	8	LLO	L	17.5V	+2.94°	-22.1°	1.2W
	11	S	L	22.6V	-13.9°	-41.1°	1.3W
R	8	S	L	21V	-8.9°	-40.7°	1.3W
	11	LLO	L	27V	-8.42°	-41.7°	1.6W
S	8	S	SLNL	15.5V	-13.1°	+10.46°	2.4W
	11	S	SLNL	21.5	-3.2°	+11.0°	3.2W
T	8	S	SENL	5V	PNA-HLO	+22.55°	2.1W
	11	LLO	L	21.5V	+8.4°	+19.6°	2.9W
U	15	LLO	SENL	6V	PNA-LLO	20.4°	4.2W

ABBREVIATION CODE	MEANING
S	Stable
LLO	Low level oscillations
HLO	High level oscillations
L	Linear
SLNL	Slightly nonlinear
SENL	Severely nonlinear
CD	Crossover distortion
PNA	Phase not available - reason
CNA	Curves not available

TABLE XII Correlation of Stability Tests

IDENTIFICATION OF AMPLIFIER	MOTOR SIZE	STABILITY FROM FREQ. RESPONSE	STABILITY FROM TRANSFER FCT. PLOT	CORRELATION CODE
A	8	U	B	B
	11	S	B	B
B	8E	B	S	B
	8I	U	NA	NA
	11	S	S	+
C	8	S	S	+
	11	S	S	+
D	8E	B	S	B
	8I	U	NA	NA
	11	S	S	+
E	8	S	S	+
	11	S	S	+
F	8	S	S	+
	11	S	S	+
G	8	S	S	+
	11	S	S	+
H	8	S	S	+
	11	S	S	+
I	8	S	S	+
	11	S	S	+
J	8	S	U	-
	11	S	U	-
K	8	U	U	+
	11E	B	B	+
	11I	S	NA	NA
L	8	U	U	+
	11E	B	B	+
	11I	B	NA	NA
M	8	S	S	+
	11	S	S	+
N	8	S	S	+
	11	S	S	+
O	15	curves not available	curves not available	NA
P	15	S	U	-
Q	8	S	S	+
	11	S	S	+
R	8	S	S	+
	11	S	S	+
S	8	S	S	+
	11E	S	S	+
	11I	B	NA	NA
T	8	S	S	+
	11	S	S	+
U	15E	B	U	B
	15I	B	NA	NA

TABLE XII (Continued)

* The letter I indicates ideal load, and the letter $\hat{E}$ indicates experimental load used in lab tests.

** B - Borderline
S - Stable
U - Unstable
NA - Not applicable

*** (+) - Plots agree
(-) - Plots disagree
B - Borderline
NA - Not applicable

VIII. EVALUATION OF SERVO AMPLIFIER PERFORMANCE

A. CRITERIA FOR EVALUATION OF SERVO AMPLIFIER/SERVOMOTOR COMBINATIONS

1. Stability Evaluations Using Motor and Amplifier Frequency Characteristics

The exact criteria for stability prediction using the frequency characteristics comparison was presented in section VII.C. Some small errors exist in the values of the curves due to measurement inaccuracies and computations. The tests were performed on, at most, a sample size of two for any given amplifier model number. Table X lists the amplifiers which were tested. Therefore, the spread of frequency characteristics for a larger sample size would be significantly greater.

All that was done in this situation was to list whether or not the amplifier/load combinations operated solidly in the stable or unstable regions. Combinations which came "close" to being stable or unstable were categorized "borderline". The definition of "close" is somewhat arbitrary, but all combinations were evaluated using the same definition. A combination is considered borderline if (1) at a crossover of the angles of Z_{12} and Z (unstable) (loop gain angle = 180°), the loop gain magnitude ($|Z_{12}|/|Z$ (unstable)$|$) is in the range of 0.8 to 1.25 or (2) when the loop gain magnitude is 1.0, the loop gain phase angle is within 20° of ± 180°.

2. Stability Evaluation Using Transfer Function Characteristics

As indicated previously, only the instabilities which cause major perturbations in the amplitude of the amplifier output will be detected on the output of the demodulator test set. Figure 30 illustrates a transfer function plot of a combination which did not show signs of oscillations while Figures 31 and 32 present X-Y plots which illustrate slight and severe oscillations, respectively.

Higher frequency (greater than 400 hertz) instabilities which cause only very small changes in carrier signal amplitude can be detected by using an oscilloscope to monitor the output voltage waveforms. Since

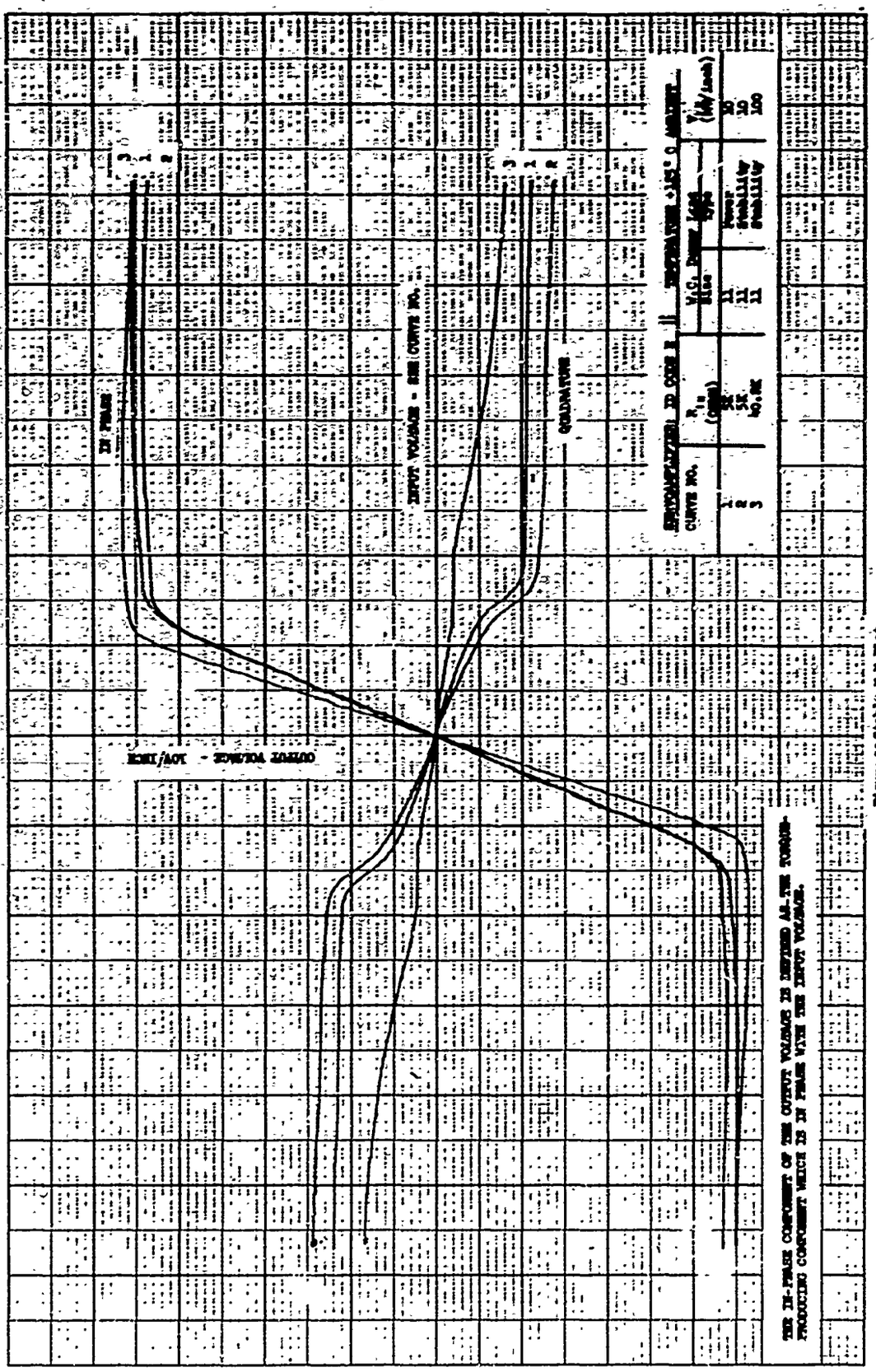

Figure 30 Typical Test Plot

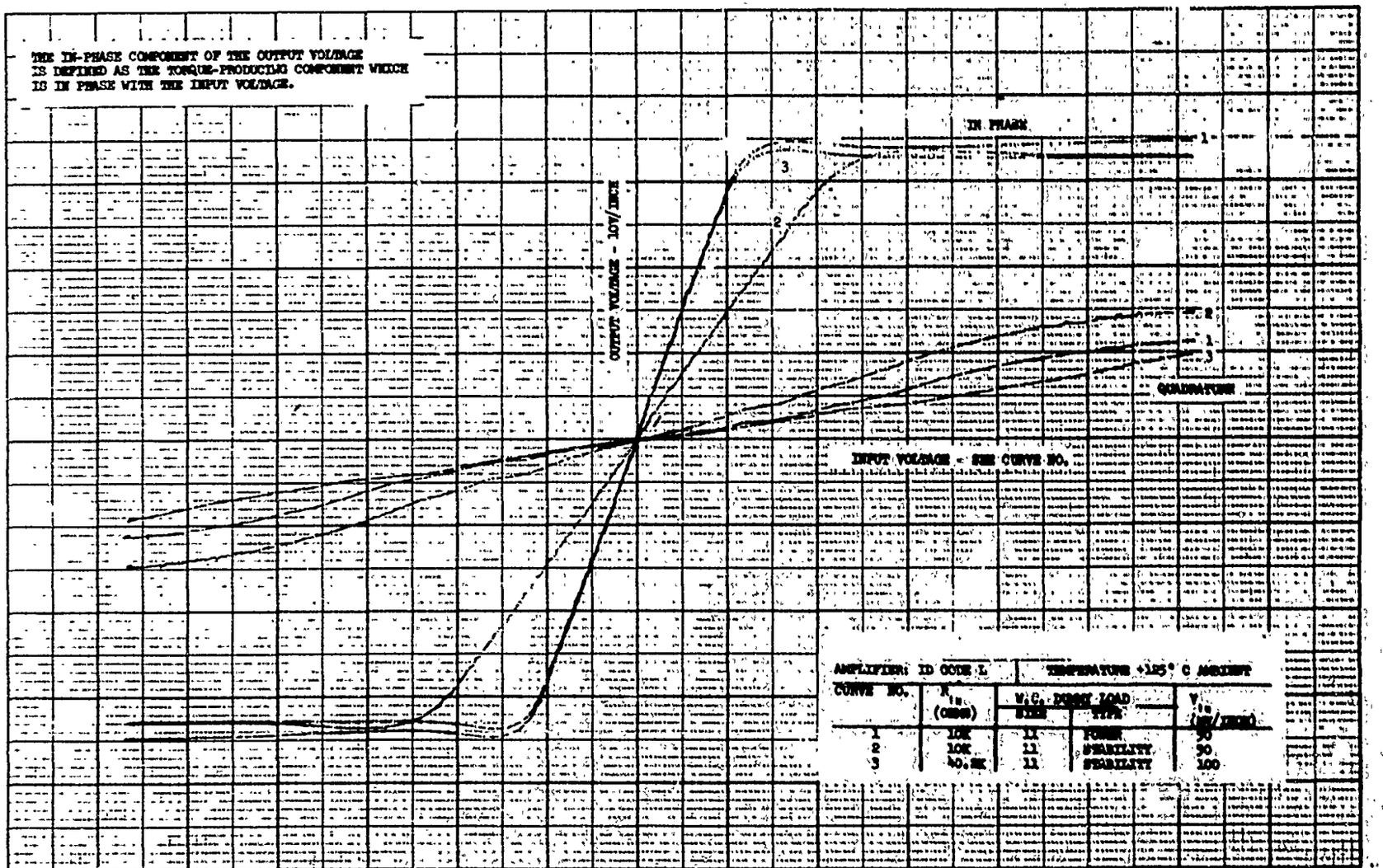

Figure 31 Low Level Oscillating XY Plot

NOT REPRODUCIBLE

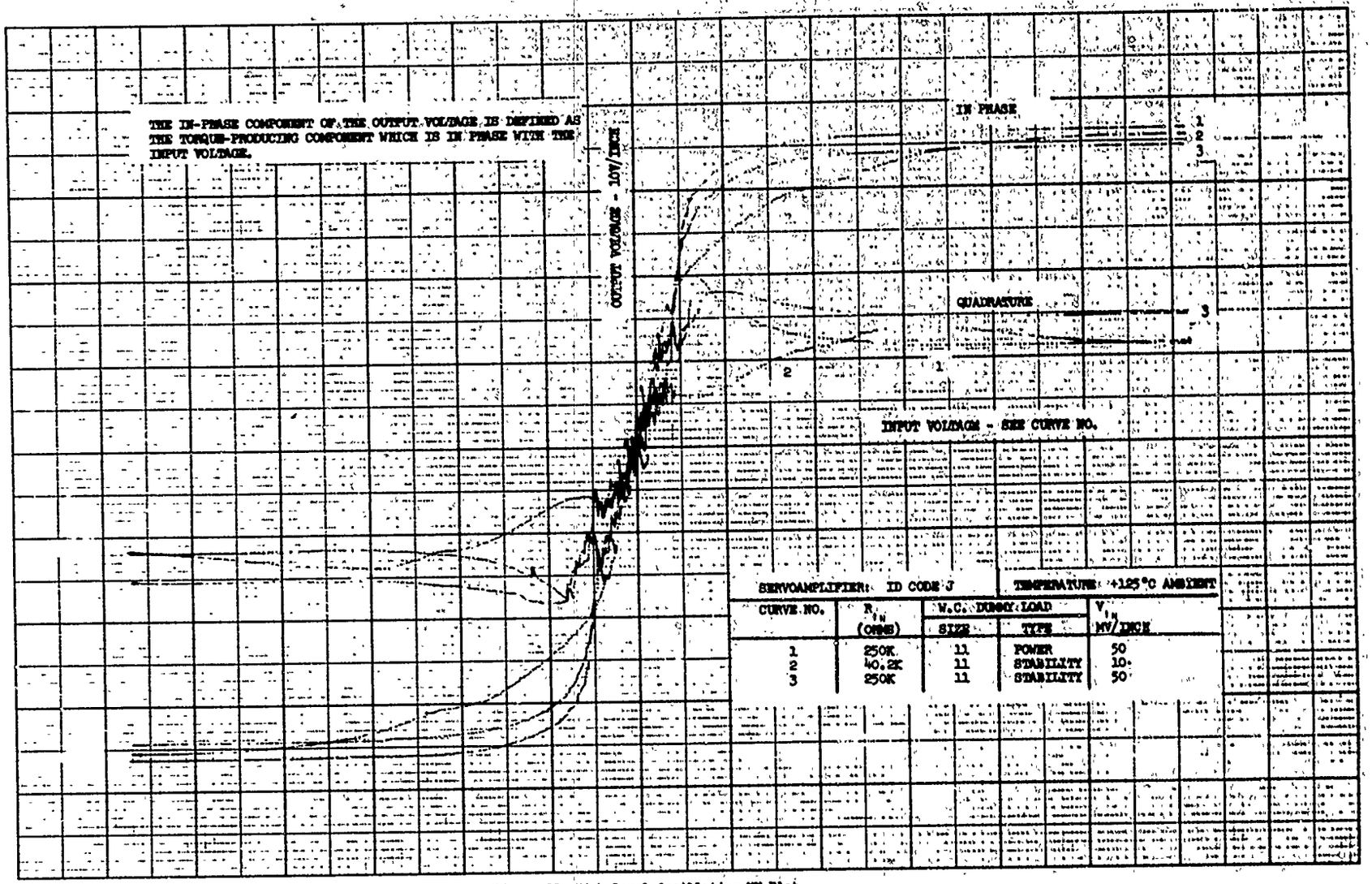

Figure 32 High Level Oscillating XY Plot

these lower amplitude oscillations did not disrupt the gain through the amplifier/load combination, these combinations were not considered important, and the outputs were not monitored with a scope.

3. Amplifier Power Output Evaluation

As mentioned previously, the worst-case power dummy load was selected to cause the minimum power output from the amplifiers. The amplifier power output was calculated from the real part of the dummy load impedance (at 400 hertz) and the in-phase component of the output voltage in the saturation region of the transfer characteristics plot. These test results represent the minimum amount of useful power (that which produces torque in the motor) which the amplifier will supply.

B. SUMMARY OF TEST RESULTS

Table XI summarizes the data taken from the transfer plots for each amplifier. Included in this table are stability and gain linearity information for the worst-case power dummy loads on the amplifiers.

Stability prediction information using both the frequency response comparison method and the transfer function characteristics is presented in Table XII along with the correlation between the two different prediction methods. Since the experimental dummy load frequency characteristics did not agree with those of the ideal dummy load at high frequencies, there occasionally appears a different stability prediction for the ideal and for the experimental load. Only the predictions from the experimental loads were used to correlate with the transfer plot stability predictions.

C. SUMMARY OF SERVO AMPLIFIER PERFORMANCE

The servo amplifier performance data is presented in Tables XI and XII. It would be more beneficial to present this data and let the reader draw his own conclusions rather than make arbitrary divisions between acceptable and unacceptable performance. However, Table XIII does make predictions of the stability of amplifiers which were tested when connected to any motor with specifications which fall in the ranges given in the recommendations (section II). It should be emphasized that these predictions are based on a very small sample size.

TABLE XIII Summary Of Amplifier Stability

IDENTIFICATION OF AMPLIFIER	MOTOR SIZE	STABILITY PERFORMANCE
A	6	B
	11	B
B	8	B
	11	S
C	8	S
	11	S
D	8	B
	11	S
E	8	S
	11	S
F	8	S
	11	S
G	8	S
	11	S
H	8	S
	11	S
I	8	S
	11	S
J	8	D
	11	D
K	8	U
	11	S
L	8	U
	11	B
M	8	S
	11	S
N	8	S
	11	S
O	15	NA
P	15	D
Q	8	S
	11	S
R	8	S
	11	S
S	8	S
	11	B
T	8	S
	11	S
U	15	B

S - Stable
B - Borderline Stability
NA - Not Available
U - Unstable
D - Disagreement in Predictions (Amplifier Oscillates)